PDGFRα and CD51 mark human Nestin+ sphere-forming mesenchymal stem cells capable of hematopoietic progenitor cell expansion

Sandra Pinho,[1,2] Julie Lacombe,[1,2] Maher Hanoun,[1,2] Toshihide Mizoguchi,[1,2] Ingmar Bruns,[1,2,4] Yuya Kunisaki,[1,2] and Paul S. Frenette[1,2,3]

[1]Ruth L. and David S. Gottesman Institute for Stem Cell and Regenerative Medicine Research, [2]Department of Cell Biology, and [3]Department of Medicine, Albert Einstein College of Medicine, Bronx, NY 10461
[4]Department of Hematology, Oncology, and Clinical Immunology, Heinrich Heine University Düsseldorf, 40225 Düsseldorf, Germany

The intermediate filament protein Nestin labels populations of stem/progenitor cells, including self-renewing mesenchymal stem cells (MSCs), a major constituent of the hematopoietic stem cell (HSC) niche. However, the intracellular location of Nestin prevents its use for prospective live cell isolation. Hence it is important to find surface markers specific for Nestin+ cells. In this study, we show that the expression of PDGFRα and CD51 among CD45− Ter119− CD31− mouse bone marrow (BM) stromal cells characterizes a large fraction of Nestin+ cells, containing most fibroblastic CFUs, mesenspheres, and self-renewal capacity after transplantation. The PDGFRα+ CD51+ subset of Nestin+ cells is also enriched in major HSC maintenance genes, supporting the notion that niche activity co-segregates with MSC activity. Furthermore, we show that PDGFRα+ CD51+ cells in the human fetal BM represent a small subset of CD146+ cells expressing Nestin and enriched for MSC and HSC niche activities. Importantly, cultured human PDGFRα+ CD51+ nonadherent mesenspheres can significantly expand multipotent hematopoietic progenitors able to engraft immunodeficient mice. These results thus indicate that the HSC niche is conserved between the murine and human species and suggest that highly purified nonadherent cultures of niche cells may represent a useful novel technology to culture human hematopoietic stem and progenitor cells.

CORRESPONDENCE
Paul S. Frenette:
paul.frenette@einstein.yu.edu

Abbreviations used: CFU-C, CFU in culture; CFU-F, fibroblastic CFU; Flt3L, Flt3 ligand; gw, gestation week; HA/TCP, hydroxyapatite/tricalcium phosphate; HSC, hematopoietic stem cell; HSPC, hematopoietic stem and progenitor cell; LepR, leptin receptor; LTC-IC, long-term culture-initiating cell; MPP, multipotent progenitor; MSC, mesenchymal stem cell; PFA, paraformaldehyde; SCF, stem cell factor; TPO, thrombopoietin.

Hematopoietic stem cells (HSCs) continuously replenish all blood cell lineages throughout their lifetime. Incipient hematopoiesis is first detected extraembryonically in the yolk sac and later in the aorta–gonad–mesonephros region, from where it moves transiently to the placenta and liver before being stabilized in the fetal BM (Wang and Wagers, 2011). In the adult stage, HSCs reside in a highly complex and dynamic microenvironment of the BM commonly referred to as the HSC niche (Schofield, 1978). The interactions between the niche constituents and HSCs ensure hematopoietic homeostasis by regulating HSC self-renewal, differentiation, and migration and by integrating neural and hormonal signals from the periphery (Méndez-Ferrer et al., 2009, 2010; Mercier et al., 2012). However, HSC maintenance and expansion ex vivo still remains challenging mainly because of our limited knowledge on the in vivo HSC niche constituents and the factors that drive HSC self-renewal.

Although the cellular constituents of the HSC niche and their role are still poorly understood, in the last decade, several putative cellular components of the murine HSC niche have been proposed, including osteoblastic, endothelial, adipocytic, and perivascular cells (Calvi et al., 2003;

S. Pinho and J. Lacombe contributed equally to this paper.

The Rockefeller University Press $30.00
J. Exp. Med. 2013 Vol. 210 No. 7 1351-1367
www.jem.org/cgi/doi/10.1084/jem.20122252

Zhang et al., 2003; Arai et al., 2004; Kiel et al., 2005; Sugiyama et al., 2006; Chan et al., 2009; Naveiras et al., 2009; Méndez-Ferrer et al., 2010; Ding et al., 2012). Multipotent BM mesenchymal stem cells (MSCs) have long been suggested to also provide regulatory signals to hematopoietic progenitors, as mixed cultures derived from the adherent fraction of the BM stroma promote the maintenance of HSCs in vitro (Dexter et al., 1977). Although numerous studies explored the ability of mesenchymal stromal cultures to support the ex vivo expansion of hematopoietic stem and progenitor cells (HSPCs), currently these systems are still insufficient to preserve primitive HSCs with long-term multilineage engraftment capacity (Chou et al., 2010; Broxmeyer, 2011). This limitation may in part be associated with the heterogeneous composition of mesenchymal stromal cell cultures. The prospective identification and functional characterization of purified naive populations of mouse and/or human BM stromal MSCs have been mired by the absence of specific cell surface markers allowing prospective isolation. Several MSC-associated antigens have been proposed (such as CD31$^-$ CD34$^-$ CD45$^-$ CD105$^+$ CD90$^+$ CD73$^+$) in cultured cells (Dominici et al., 2006). Nevertheless, these markers are not homogeneously expressed across cultures, varying with isolation protocols and passage and therefore not necessarily representative of MSCs in vivo (Bianco et al., 2013; Frenette et al., 2013). Very few MSC-associated antigens have been validated using rigorous transplantation assays (Sacchetti et al., 2007; Méndez-Ferrer et al., 2010). In the mouse BM, the expression of the intermediate filament protein Nestin characterizes a rare population of multipotent MSCs in close contact with the vasculature and HSCs. Nestin$^+$ stromal cells contain all of the fibroblastic CFU (CFU-F) activity within the mouse BM and the exclusive capacity to form clonal nonadherent spheres in culture. The selective ablation of mouse Nestin$^+$ cells (Méndez-Ferrer et al., 2010) or CXCL12-abundant reticular (CAR) cells (Omatsu et al., 2010) led to significant alterations in the BM HSC and progenitor maintenance. Serial transplantation analyses revealed that Nestin$^+$ cells are able to self-renew and generate hematopoietic activity in heterotopic bone ossicle assays (Méndez-Ferrer et al., 2010). This potential was also associated with a CD45$^-$ Tie2$^-$ αV$^+$ CD105$^+$ CD90$^-$ subset from the fetal mouse bone (Chan et al., 2009). In the adult mouse BM, PDGFRα$^+$ Sca1$^+$ CD45$^-$ Ter119$^-$ cells were also shown capable to give rise to osteoblasts, reticular cells, and adipocytes in vivo upon transplantation into irradiated mice (Morikawa et al., 2009). However, human BM MSCs are still retrospectively isolated based on plastic adherence (Friedenstein et al., 1970; Pittenger et al., 1999). Human CD45$^-$ CD146$^+$ self-renewing osteoprogenitors isolated from stromal cultures containing all the human BM CFU-F activity were shown capable of generating a heterotopic BM niche in an s.c. transplantation model (Sacchetti et al., 2007). However, a recent study showed that human CD45$^-$ CD271$^+$ CD146$^{-/low}$ BM cells also possess these capacities (Tormin et al., 2011).

Because Nestin is an intracellular protein, its identification in nontransgenic mice requires cell permeabilization, which precludes prospective isolation of live cells. In this study, we have evaluated putative cell surface MSC markers to identify a stromal population equivalent to Nestin$^+$ cells in the mouse and human BM. Our results show that the combination of PDGFRα and CD51 identify a large subset of perivascular Nestin$^+$ cells that is highly enriched in MSC and HSC niche activities in both species. Furthermore, we show that PDGFRα$^+$ CD51$^+$ stromal cells isolated from human BM can also form self-renewing clonal mesenspheres capable of transferring hematopoietic niche activity in vivo and support the ex vivo maintenance and expansion of human HSPCs in a dose-dependent manner.

RESULTS

PDGFRα and CD51 are highly expressed on Nes-GFP$^+$ cells

To identify cell surface marker defining Nestin$^+$ cells, we used microarray data (Méndez-Ferrer et al., 2010) and previously published MSC markers. Among nonhematopoietic (CD45$^-$ Ter119$^-$) and nonendothelial (CD31$^-$) Nes-GFP$^+$ cells dissociated with collagenase IV, PDGFRα and αV integrin (CD51) were highly and uniformly expressed by BM Nestin$^+$ cells (82 ± 3% and 79 ± 3%, respectively; Fig. 1, A and B). Another putative MSC marker, endoglin (CD105), was also expressed by 65 ± 3% of Nestin$^+$ cells. Other conventional mesenchymal lineage markers were heterogeneously expressed (CD29, CD44, CD61, CD130, and P75) or restricted to a small subset (<15%) of Nestin$^+$ cells (CD10, CD90, CD166, and CD133). Ng2 (Ozerdem et al., 2001) and CD146 (Li et al., 2003; Sacchetti et al., 2007), two known perivascular markers were expressed in a very small fraction of BM Nestin$^+$ cells (<10%). Surprisingly, the putative MSC marker Sca-1 (Meirelles and Nardi, 2003; Morikawa et al., 2009) was expressed only in a small subset (6 ± 1%) of the BM Nestin$^+$ population (Fig. 1, A and B). As expected, various hematopoietic markers (c-Kit, CD135, CD34, CD41, CD48, and CD11b) were absent or expressed by <10% of Nestin$^+$ cells (Fig. 1 A).

We next conducted a thorough analysis of the population labeled by the combination of the two most highly expressed antigens (PDGFRα and CD51) within the Nes-GFP population (Fig. 1 C) or within the total stromal population (Fig. 1 D) to test whether these markers faithfully define Nes-GFP$^+$ cells. PDGFRα and CD51 double-positive cells comprised a major subset of the Nes-GFP$^+$ population (~60%; Fig. 1 C). By gating first on PDGFRα$^+$ CD51$^+$ cells, they represented a rare fraction (~2%) of the CD45$^-$ Ter119$^-$ CD31$^-$ stromal population but were highly enriched in Nes-GFP$^+$ cells (~75%; Fig. 1 D). Endogenous *Nestin* expression, as detected by real-time PCR, was also enriched in stromal PDGFRα$^+$ CD51$^+$ cells compared with single-positive or negative stromal cells (Fig. 1 E).

Stromal PDGFRα$^+$ CD51$^+$ cells express high levels of HSC niche genes

Nestin$^+$ cells express high levels of HSC maintenance genes such as the chemokine *Cxcl12*, *Vcam1* (*vascular cell adhesion molecule-1*), *Angpt1* (*angiopoietin-1*), *Scf* (*stem cell factor*), and *Opn*

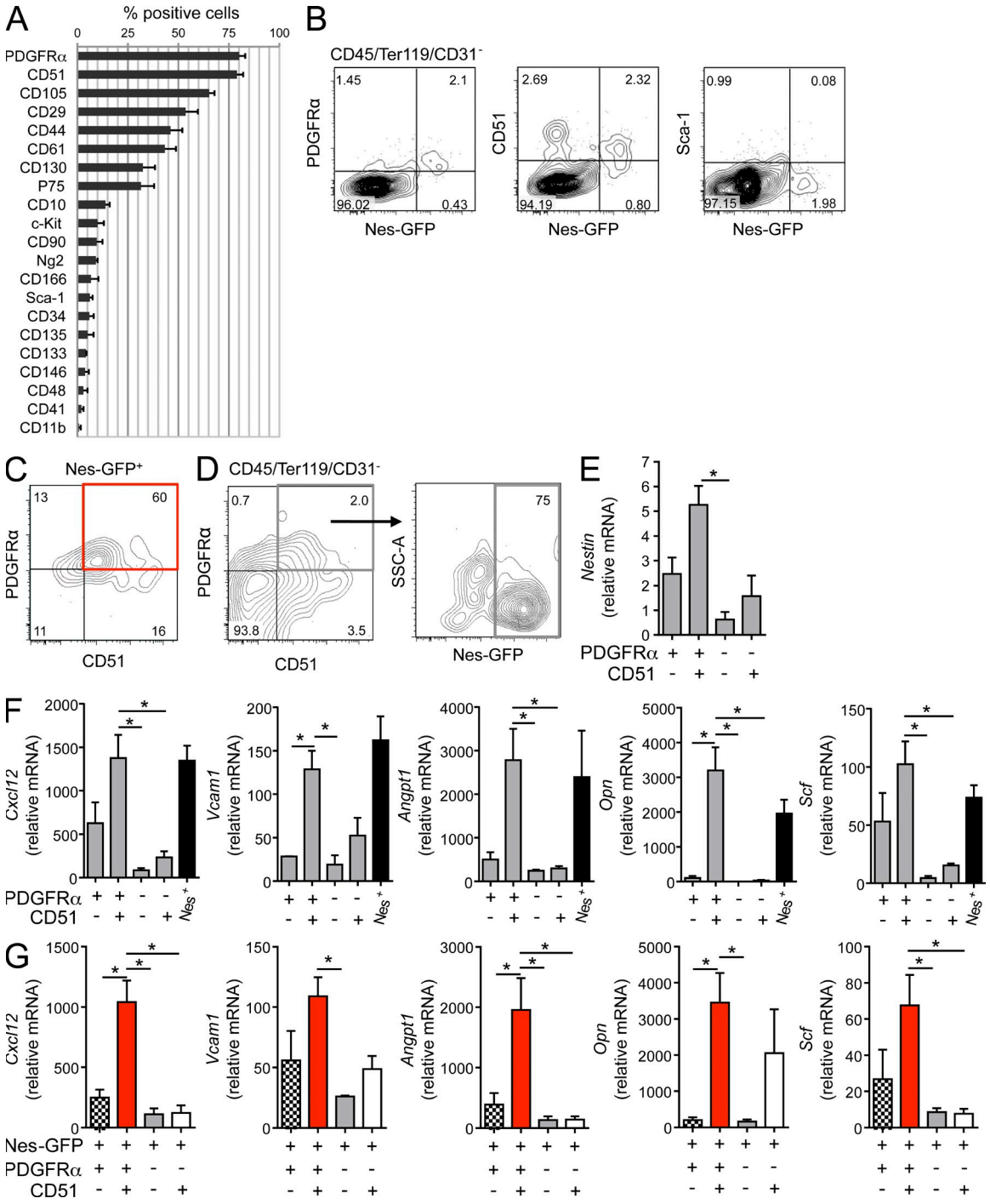

Figure 1. Mouse BM PDGFRα⁺ CD51⁺ cells constitute an enriched population of Nes-GFP⁺ cells. (A) Stromal (CD45⁻ Ter119⁻ CD31⁻) Nestin⁺ cells were isolated from Nes-*Gfp* transgenic mice and analyzed for the expression of the indicated cell surface markers by flow cytometry. $n = 3$–9. (B) Expression of PDGFRα and Nes-GFP, CD51 and Nes-GFP, and Sca-1 and Nes-GFP markers on CD45⁻ Ter119⁻ CD31⁻ stromal cells as determined by flow cytometry. (C) PDGFRα and CD51 expression on Nes-GFP⁺ BM cells. (D) Stromal PDGFRα⁺ CD51⁺ cells were analyzed for Nes-GFP expression by flow cytometry. Numbers in B–D indicate the percentage of positive cells present in the indicated gates. Data are representative of three to nine independent analyses with comparable results. (E) Stromal PDGFRα⁺ CD51⁺ cells were isolated from the BM of C57BL/6 wild-type mice, and *Nestin* mRNA levels were measured by real-time PCR. (F and G) Stromal BM cells from wild-type mice (F) and stromal Nestin⁺ cells from Nes-*Gfp* transgenic mice (G) were sorted based on expression of PDGFRα and CD51 and the expression of the indicated genes assessed by real-time PCR. GFP⁺ cells from Nes-*Gfp* transgenic mice were compared with BM cell populations in F. Data are from three to eight independent sorting experiments. *, $P < 0.05$; unpaired two-tailed Student's *t* test. All error bars indicate SEM.

(*osteopontin*; Méndez-Ferrer et al., 2010). We sorted PDGFRα and CD51 double- and single-positive subsets among total stromal cells (CD45$^-$ Ter119$^-$ CD31$^-$) from wild-type mice to evaluate their niche properties alongside Nes-GFP$^+$ cells as positive control. We found that PDGFRα and CD51 double-positive cells consistently enriched for the highest levels of HSC regulatory genes (Fig. 1 F). The addition or substitution of CD105, the third most highly expressed marker, to PDGFRα and CD51 did not further enrich in HSC niche activity (not depicted). Within the Nes-GFP$^+$ population, the PDGFRα$^+$ CD51$^+$ subset also expressed the highest levels of these factors (Fig. 1 G), suggesting that the HSC niche activity of stromal Nestin$^+$ cells is enriched in the PDGFRα$^+$ CD51$^+$ subpopulation. To confirm this finding, we further compared the expression levels between PDGFRα$^+$ CD51$^+$ cells and the small fraction of Nes-GFP$^+$ cells that were not double positive for PDGFRα and CD51 (Fig. 2). Approximately 1.3% of the cells not expressing both PDGFRα and CD51 (gray gate) were Nes-GFP$^+$ (blue gate) and expressed significantly lower levels of HSC maintenance factors (Fig. 2, A and B) compared with the entire PDGFRα$^+$ CD51$^+$ population (red gate), of which ∼75% were Nes-GFP$^+$ (green gate). Furthermore, our gene expression analysis showed that within the PDGFRα$^+$ CD51$^+$ population, a small fraction of Nes-GFP$^-$ cells (∼25%; Fig. 2 A, purple gate) also expressed meaningful levels of HSC niche genes, notably *Opn* and *Scf* (Fig. 2 C). All together, these results show that PDGFRα$^+$ CD51$^+$ stromal cells express the key HSC niche genes contained in Nestin$^+$ cells and suggest that this population may represent a suitable alternative to prospectively isolate niche cells.

PDGFRα$^+$ CD51$^+$ BM stromal cells recapitulate the MSC activity of Nestin$^+$ cells

Our previous studies have revealed that Nes-GFP$^+$ cells contain all of the MSC activity in the BM, as determined by their exclusive ability to form CFU-Fs and mesenspheres that can self-renew in vivo (Méndez-Ferrer et al., 2010). Because both MSC and HSC niche activities are very rare in BM, and likely are derived from a subset of Nes-GFP$^+$ cells, it remains possible that the two activities are not conferred by the same cell. Having found that niche activity was enriched in PDGFRα$^+$ CD51$^+$ cells, which comprised 60% of Nes-GFP$^+$ cells, we next tested whether MSC activity co-segregated with niche function. CFU-F assays of sorted double- and single-positive

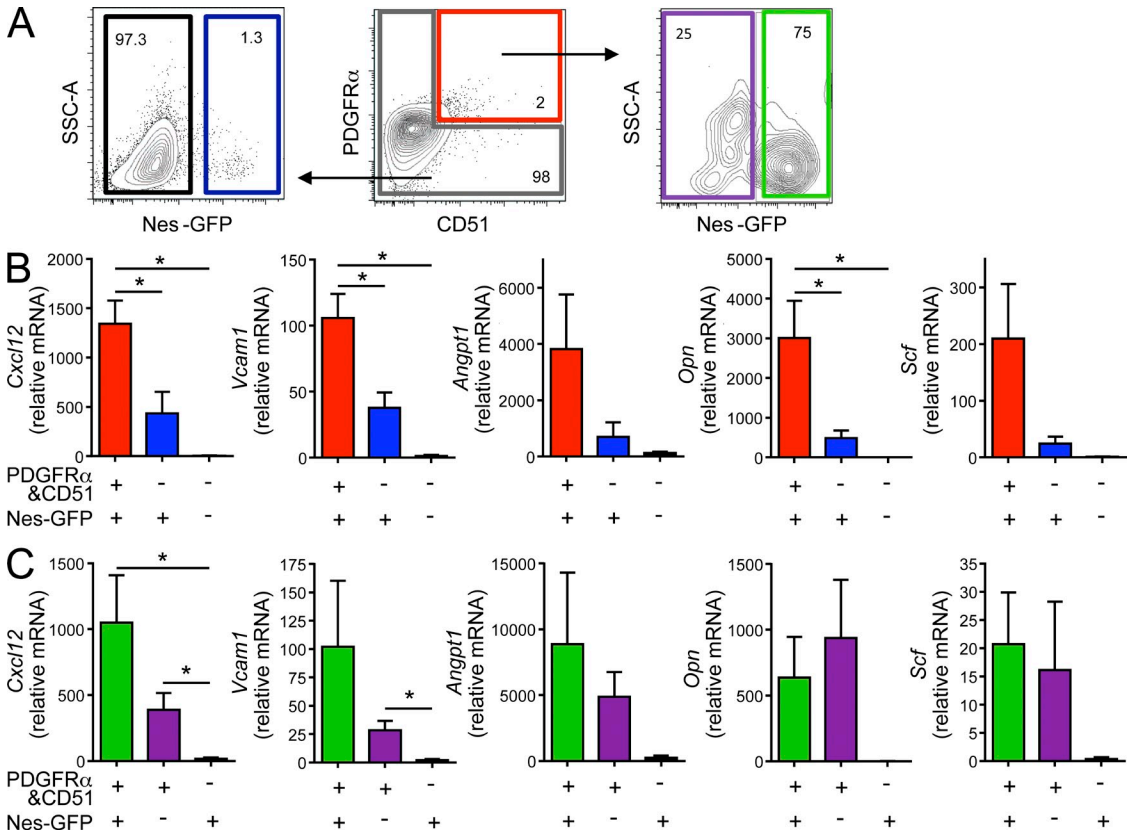

Figure 2. Stromal PDGFRα$^+$ CD51$^+$ cells express high levels of HSC regulatory genes in contrast to the small fraction of PDGFRα$^-$ CD51$^-$ Nes-GFP$^+$ cells. (A) CD45$^-$ Ter119$^-$ CD31$^-$ stromal cells from Nes-*Gfp* transgenic mice were gated as shown: PDGFRα$^+$ CD51$^+$ (middle; red), PDGFRα$^-$ CD51$^-$ (middle; gray), PDGFRα$^-$ CD51$^-$ Nes-GFP$^-$ (left; black), PDGFRα$^-$ CD51$^-$ Nes-GFP$^+$ (left; blue), PDGFRα$^+$ CD51$^+$ Nes-GFP$^-$ (right; purple), and PDGFRα$^+$ CD51$^+$ Nes-GFP$^+$ (right; green). (B and C) Stromal PDGFRα and CD51 BM cell populations were sorted according to the gates in A and analyzed for expression of the HSC regulatory genes *Cxcl12*, *Vcam1*, *Angpt1*, *Opn*, and *Scf* by real-time PCR analysis. $n = 3$ independent sorting experiments. *, $P < 0.05$; unpaired two-tailed Student's *t* test. All error bars indicate SEM.

fractions revealed that mesenchymal progenitor activity was largely confined to the stromal PDGFRα$^+$ CD51$^+$ fraction (Fig. 3 A). In addition, PDGFRα$^+$ CD51$^+$ cells, but not other stromal subpopulations, plated at clonal densities (<500 cells/cm^2) or by single-cell FACS sorting deposition were able to form nonadherent primary spheres with the same efficiency as Nes-GFP$^+$ cells (Fig. 3 B). When dissociated, these spheres could be passaged and formed secondary spheres, demonstrating the in vitro self-renewal capacity of PDGFRα$^+$ CD51$^+$ cells (not depicted). In contrast, the rare and small spheres (<40 µm in diameter) forming from PDGFRα$^+$ CD51$^-$ and PDGFRα$^-$ CD51$^+$ subpopulations (Fig. 3 B) did not have the capacity to form secondary spheres in culture. When PDGFRα$^+$ CD51$^+$ cells were isolated from Nes-*Gfp* mice, the majority of the clonal spheres (~40–130 µm in diameter) retained Nes-GFP expression until ~1.5 wk in culture (Fig. 3 C). Using conventional adherent MSC culture conditions (Phinney et al., 1999; Pittenger et al., 1999), sorted PDGFRα$^+$ CD51$^+$

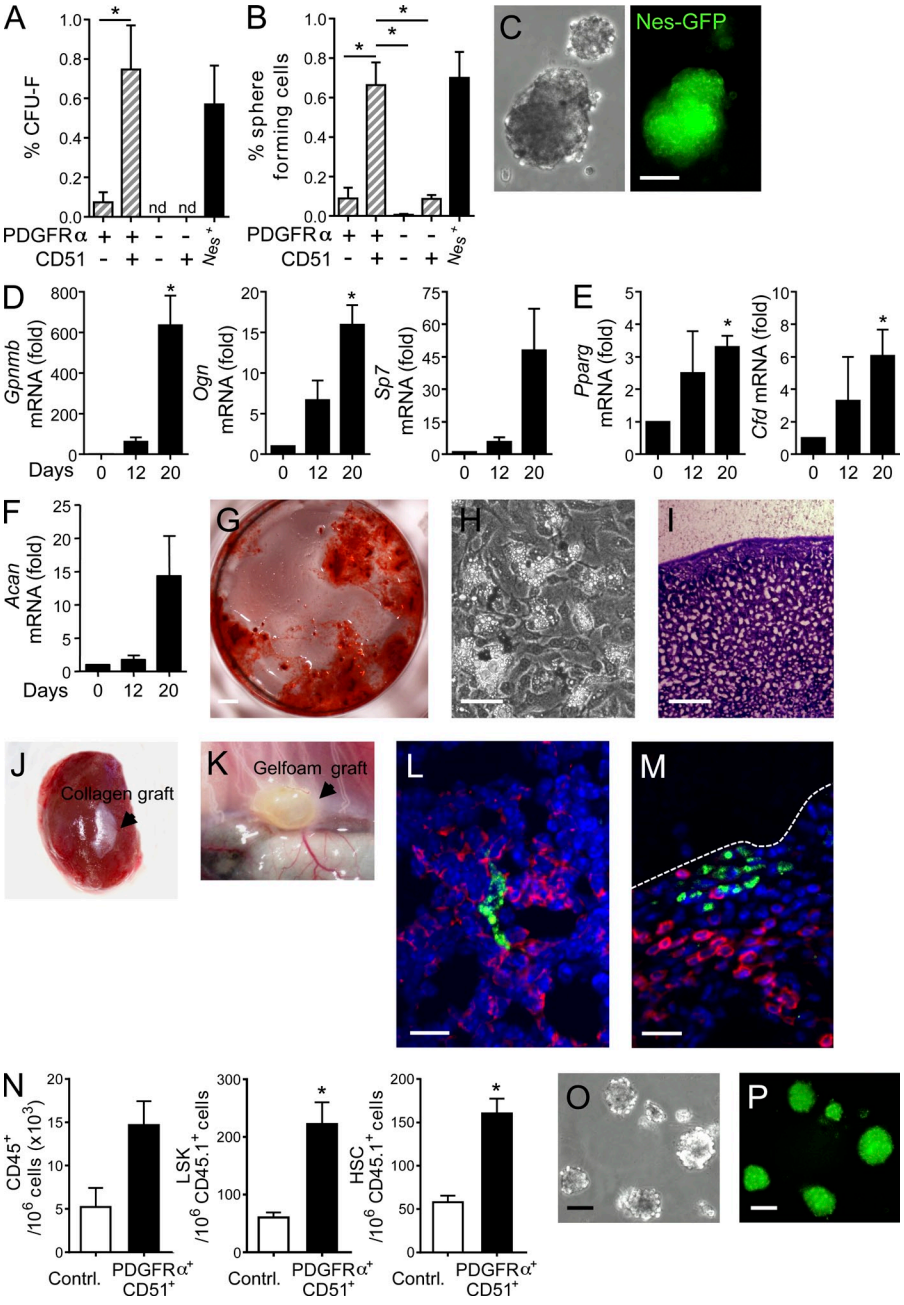

Figure 3. PDGFRα$^+$ CD51$^+$ BM stromal cells contain the HSC niche activity observed in Nes-GFP$^+$ MSCs. (A–I) CD45$^-$ Ter119$^-$ CD31$^-$ stromal cells were sorted based on expression of PDGFRα and CD51 and characterized in vitro for MSC activity. (A and B) Cells were plated at clonal densities, and the percentage of CFU-F (A) and self-renewing spheres (B) in sorted PDGFRα$^+$ CD51$^+$ cells and other subsets isolated from wild-type mice, alongside GFP$^+$ cells from Nes-*Gfp* mice, were determined. n = 3–5 CFU-F and n = 4–9 clonal sphere independent sorting experiments; nd, not detectable. (C) GFP expression of stromal PDGFRα$^+$ CD51$^+$ self-renewing clonal spheres isolated from Nes-*Gfp* mice after 1.5 wk in culture. (D–I) Multilineage differentiation capacity of PDGFRα$^+$ CD51$^+$ cells. PDGFRα$^+$ CD51$^+$ spheres were plated in differentiation conditions, and the differentiation kinetic was evaluated by real-time PCR for the expression of osteogenic (*Gpnmb*, *Ogn*, and *Sp7*; D), adipogenic (*Pparg* and *Cfd*; E), and chondrogenic (*Acan*; F) lineage-specific genes at days 0, 12, and 20. n = 3. Fully differentiated phenotypes of PDGFRα$^+$ CD51$^+$ spheres were tested by Alizarin Red S (osteogenic; G), lipid vacuole accumulation (adipogenic; H), and Toluidine Blue (chondrogenic; I) staining. (J–M) Single clonal PDGFRα$^+$ CD51$^+$ spheres isolated from Nes-*Gfp* mice were incorporated into collagen (J and L) or gelfoam grafts (K and M) and transplanted under the renal capsule or s.c. into recipient mice, respectively. (L and M) 8 wk after implantation, the presence of Nes-GFP$^+$ cells (green) and host CD45$^+$ hematopoietic cells (red) was investigated by immunofluorescence. Cell nuclei were stained with DAPI (blue). The white dashed line delineates the gelfoam graft in M. (N) The numbers of engrafted CD45$^+$ (left), CD45$^+$ CD41$^-$ Lin$^-$ Sca1$^+$ c-Kit$^+$ (middle), and CD45$^+$ CD41$^-$ Lin$^-$ Sca1$^+$ c-Kit$^+$ CD48$^-$ CD150$^+$ HSCs (right) inside PDGFRα$^+$ CD51$^+$ renal capsule ectopic grafts and empty control grafts were analyzed by flow cytometry. (O and P) Brightfield (O) and fluorescence Nes-GFP$^+$ (green; P) images of secondary PDGFRα$^+$ CD51$^+$ clonal spheres derived from dissociated gelfoam grafts 8 wk after transplantation. Bars: (C) 100 µm; (G) 500 µm; (H, I, and L) 50 µm; (M, O, and P) 20 µm. *, $P < 0.05$; unpaired two-tailed Student's t test. All error bars indicate SEM.

cells rapidly down-regulated HSC maintenance gene expression along with Nes-GFP (not depicted).

Clonally expanded PDGFRα$^+$ CD51$^+$ spheres plated into in vitro mesenchymal lineage differentiation conditions exhibited robust tri-lineage potential, with up-regulation of osteoblastic (Fig. 3 D), adipocytic (Fig. 3 E), and chondrocytic (Fig. 3 F) differentiation genes during a 12–20-d period. Multilineage differentiation was confirmed by morphological and histochemical characterization of mature osteoblastic (Fig. 3 G), adipocytic (Fig. 3 H), and chondrocytic (Fig. 3 I) lineage phenotypes after >30 d in culture.

Self-renewing murine PDGFRα$^+$ CD51$^+$ cells are able to transfer hematopoietic niche activity in vivo

To examine whether PDGFRα$^+$ CD51$^+$ cells were capable to self-renew in vivo and transfer hematopoietic activity (Sacchetti et al., 2007; Méndez-Ferrer et al., 2010), we used two different transplantation approaches to deliver single clonal PDGFRα$^+$ CD51$^+$ spheres derived from Nes-*Gfp* mice. In the first approach, single spheres were incorporated into collagen grafts and implanted under recipients' kidney capsules (Fig. 3, J and L), and alternatively, spheres were implanted s.c. within collagen gelfoam grafts (Fig. 3, K and M). 8 wk after transplantation, Nes-GFP$^+$ cells were detected inside the grafts and in close contact with host CD45$^+$ hematopoietic cells recruited in the extramedullary microenvironment (Fig. 3, L and M). In contrast, PDGFRα$^-$ CD51$^+$ and PDGFRα$^+$ CD51$^-$ spheres did not display any self-renewing Nes-GFP$^+$ cells, and very few CD45$^+$ cells were present inside the graft (not depicted). Controls included nontransplanted kidney capsules and grafts without stromal cells that only showed very rare CD45$^+$ inflammatory cells.

To further determine whether the ectopic grafts loaded with mouse PDGFRα$^+$ CD51$^+$ cells could provide a functional niche for HSCs to engraft, we quantified by FACS analysis the presence of phenotypic HSCs (Fig. 3 N). We used CD45.1$^+$ congenic recipient mice to ensure that the hematopoietic cells inside the grafts were not derived from the donor transplanted cells (isolated from CD45.2 mice). There was a trend toward a higher frequency of CD45.1$^+$ cells in the PDGFRα$^+$ CD51$^+$ grafts compared with control grafts ($P = 0.06$). Furthermore, the frequency of phenotypic HSC and progenitor cells defined as CD41$^-$ Lin$^-$ Sca1$^+$ c-Kit$^+$ or CD41$^-$ Lin$^-$ Sca1$^+$ c-Kit$^+$ CD48$^-$ CD150$^+$ in the PDGFRα$^+$ CD51$^+$ grafts was ∼3.7- and 2.8-fold higher than in the control group, respectively (Fig. 3 N). These results indicate that PDGFRα$^+$ CD51$^+$ cells are able to recreate a BM microenvironment able to recruit circulating HSCs into ectopic grafts.

To investigate whether in vivo transplanted PDGFRα$^+$ CD51$^+$ cells maintained their stem cell properties, we tested their ability to form secondary spheres. 8 wk after transplantation, grafts were collected and dissociated into single-cell suspensions. These cells were able to give rise to secondary clonal spheres (Fig. 3 O) that retained Nes-GFP expression (Fig. 3 P), providing further evidence of their self-renewing capacity. Thus, these results support the idea that HSC niche and MSC activities likely co-segregate in the BM.

Relationship between Nestin$^+$, PDGFRα$^+$ CD51$^+$ MSCs, and other putative niche cells

A previous study has suggested that PDGFRα$^+$ Sca-1$^+$ (PαS) cells comprise MSCs in the BM (Morikawa et al., 2009). However, we found that Sca-1 was not expressed on the vast majority of Nestin$^+$ cells (Figs. 1 A and 4, A and B), suggesting that MSC activity in the BM lay outside of the PαS population. We hypothesized that the discrepancy between these results could originate from how cells were harvested because Morikawa et al. (2009) and Houlihan et al. (2012) isolated stromal cells from crushed bones and discarded the BM fraction. Indeed, we detected a stromal Nes-GFP$^+$ resident population in compact bone, of which ∼30% expressed Sca-1. In bone, Nestin$^+$ and PαS cells overlapped (∼23% of PαS cells are Nestin$^+$) and enriched for CFU-F activity (Fig. 4, C–E). Interestingly, PDGFRα$^+$ CD51$^+$ markers also label 45 ± 5% of Nes-GFP$^+$ cells in bone (not depicted). These results suggest that PDGFRα$^+$ CD51$^+$ cells (or Nestin$^+$ cells) are distinct from PαS cells in the BM and that PαS population is enriched in MSC activity in bone but not in BM.

Recent data have indicated that perivascular cells expressing leptin receptor (LepR) are the main source of SCF in the BM and that these cells are distinct from Nestin$^+$ cells (Ding et al., 2012). However, Nestin$^+$ cells (Méndez-Ferrer et al., 2010) and PDGFRα$^+$ CD51$^+$ cells (Fig. 1 F) express high levels of *Scf*, suggesting some overlap between Nestin$^+$ (PDGFRα$^+$ CD51$^+$) and LepR$^+$ cells. We intercrossed LepR-*cre* knock-in mice with LSL-td*tomato* reporter and Nes-*Gfp* mice to evaluate this possibility directly. Indeed, we found that BM LepR$^+$ cells largely overlap with Nes-GFP$^+$ (80 ± 7%; Fig. 4 F) and PDGFRα$^+$ CD51$^+$ populations (63 ± 8%; Fig. 4 G). Within the total Nes-GFP$^+$ population, LepR$^+$ cells also represent a major fraction (77 ± 6%; Fig. 4 F) associated with the double-positive PDGFRα$^+$ CD51$^+$ subset of Nestin$^+$ cells (Fig. 4 H). In keeping with their overlap with Nestin$^+$ and PDGFRα$^+$ CD51$^+$ cells, LepR$^+$ cells also contained CFU-F activity (Fig. 4 I).

PDGFRα and CD51 identify Nestin$^+$ cells in the human fetal BM

The identification of surface markers representing Nes-GFP$^+$ cells gave an opportunity to investigate whether a similar stromal population was present in the human BM. A population of human Nestin$^+$ cells with similar morphology to murine cells has indeed been observed in the human adult BM (Ferraro et al., 2011) and cultured adherent BM stromal cells (Schajnovitz et al., 2011). In keeping with these results, we observed in the developing human fetal BM the presence of elongated, pericyte-like Nestin$^+$ cells organized in elongated logettes surrounded by forming cartilaginous bone (Fig. 5, A–F). Human Nestin$^+$ cells were distinct from the vascular endothelial cells because they did not express VE-cadherin (Fig. 5 C); however, they showed a perivascular distribution in regions close to the bone (Fig. 5 F) or within the BM parenchyma in close contact with α-smooth muscle actin–positive vasculature (Fig. 5 D). Immunostaining for human hematopoietic lineage (Lin) markers (CD2, CD3, CD14, CD16, CD19, CD56, and CD235a),

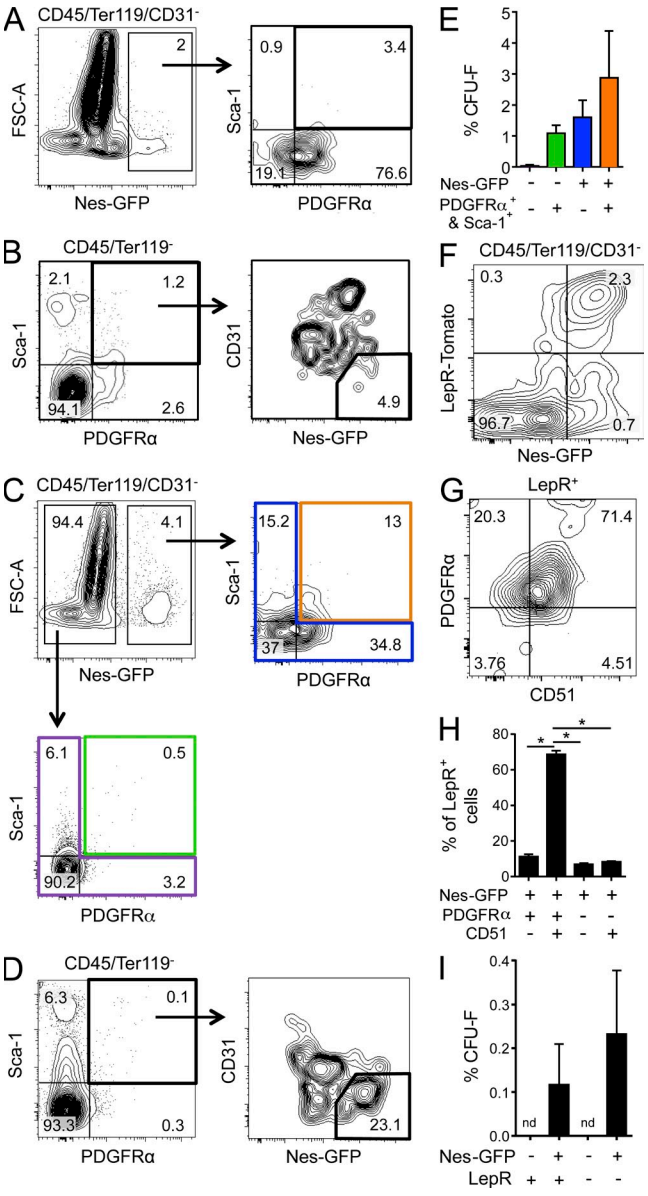

Figure 4. Overlap between Nestin⁺ and PDGFRα⁺ CD51⁺ cells with PαS and LepR⁺ cells. (A–D) The relationship between PαS and Nes-GFP⁺ cells in the mouse BM (A and B) and compact bone (C and D) was analyzed by flow cytometry. (E) CFU-F activity of sorted PαS cells and negative subsets isolated from compact bone Nes-GFP⁺ or Nes-GFP⁻ cells was analyzed after 14 d in culture. $n = 3$ independent sorting experiments. (F–H) Flow cytometry analysis of BM LepR-*Cre*/LSL-*tdtomato*/Nes-*Gfp* mice. (F) Expression of LepR and Nes-GFP markers on CD45⁻ Ter119⁻ CD31⁻ BM stromal cells determined by flow cytometry. (G) PDGFRα and CD51 expression on stromal LepR⁺ BM cells. (H) PDGFRα and CD51 cells isolated from the Nes-GFP⁺ population were analyzed for LepR expression by flow cytometry. Numbers in A–D, F, and G indicate the percentage of positive cells present in the indicated gates. (I) CFU-F activity of BM stromal cells sorted based on the expression of LepR and Nes-GFP. nd, not detectable; $n = 3$ independent experiments. *, $P < 0.05$; unpaired two-tailed Student's *t* test. All error bars indicate SEM.

CD38, and CD34 showed that Nestin⁺ cells are also in close contact with Lin⁻ CD38⁻ CD34⁺ HSC/progenitor cells in the fetal human BM (Fig. 5 E). Immunofluorescence analyses for PDGFRα and CD51 expression revealed colocalization with Nestin⁺ cells in the human fetal BM (Fig. 5 F) as in the mouse BM. In the developing human BM (15–20 gestation weeks [gw]), we found that the double-positive PDGFRα⁺ CD51⁺ cells comprised ~6.0 ± 1.6% of the stromal (CD45⁻ CD235a⁻ CD31⁻) population (Fig. 5, G and H). These PDGFRα⁺ CD51⁺ stromal cells were also present in the adult human BM, albeit at a lower frequency (<1%) than fetal BM (Fig. 5 H). Cell sorting of stromal cells expressing PDGFRα and/or CD51 revealed robust *NESTIN* expression in PDGFRα⁺ cells (Fig. 5 I). Freshly isolated human fetal PDGFRα⁺ CD51⁺ cells expressed high levels of HSC maintenance genes (*CXCL12*, *VCAM1*, *ANGPT1*, *OPN*, and *SCF*; Fig. 5 J), suggesting that PDGFRα and CD51 also define a stromal population with HSC niche activity in human BM.

Human fetal PDGFRα⁺ CD51⁺ cells are bona fide MSCs

To test whether PDGFRα⁺ CD51⁺ cells exhibit features of MSCs, we evaluated CFU-F content in double- and single-positive fractions and found that the highest clonogenic capacity was in the PDGFRα⁺ CD51⁺ subpopulation (Fig. 6 A). Furthermore, sorted human PDGFRα⁺ CD51⁺ cells were able to efficiently form nonadherent spheres in comparison with other stromal subpopulations (Fig. 6, B–D), when plated at clonal densities using the same condition as for the murine spheres. 1 wk after culture, human fetal and adult spheres continued to express PDGFRα, CD51, and NESTIN homogeneously, as seen by immunofluorescence analysis (Fig. 6 D). Human clonal PDGFRα⁺ CD51⁺ spheres were able to efficiently self-renew in vitro, forming secondary spheres upon dissociation that retain PDGFRα⁺ CD51⁺ expression in culture (not depicted). Clonally expanded fetal human PDGFRα⁺ CD51⁺ cells were also capable of robust tri-lineage differentiation into osteoblastic (Fig. 6, E and H), adipocytic (Fig. 6, F and I), and chondrocytic (Fig. 6, G and J) mesenchymal lineages, further demonstrating their MSC identity.

Human PDGFRα⁺ CD51⁺ BM cells are a small subset of CD146⁺ cells, enriched for MSC and niche activities

Because culture-expanded human CD146⁺ osteoprogenitor cells were previously shown to be highly enriched in CFU-F activity and capable of establishing the hematopoietic microenvironment in a xenotransplantation model (Sacchetti et al., 2007), we evaluated the relationship between stromal PDGFRα⁺ CD51⁺ and CD146-expressing cells. We found that stromal PDGFRα⁺ CD51⁺ also expressed CD146 homogeneously; however, only a small fraction (~16%) of the stromal CD146⁺ cells were PDGFRα⁺ CD51⁺ (Fig. 7 A), as tested in 15–20-gw human fetal BM samples. Interestingly, although both PDGFRα⁺ CD51⁺ and CD146⁺ populations expressed HSC niche genes, the PDGFRα⁺ CD51⁺ population was particularly enriched, notably for *CXCL12* (Fig. 7 B). *OPN* was highly expressed in both stromal populations. Furthermore, the gene expression

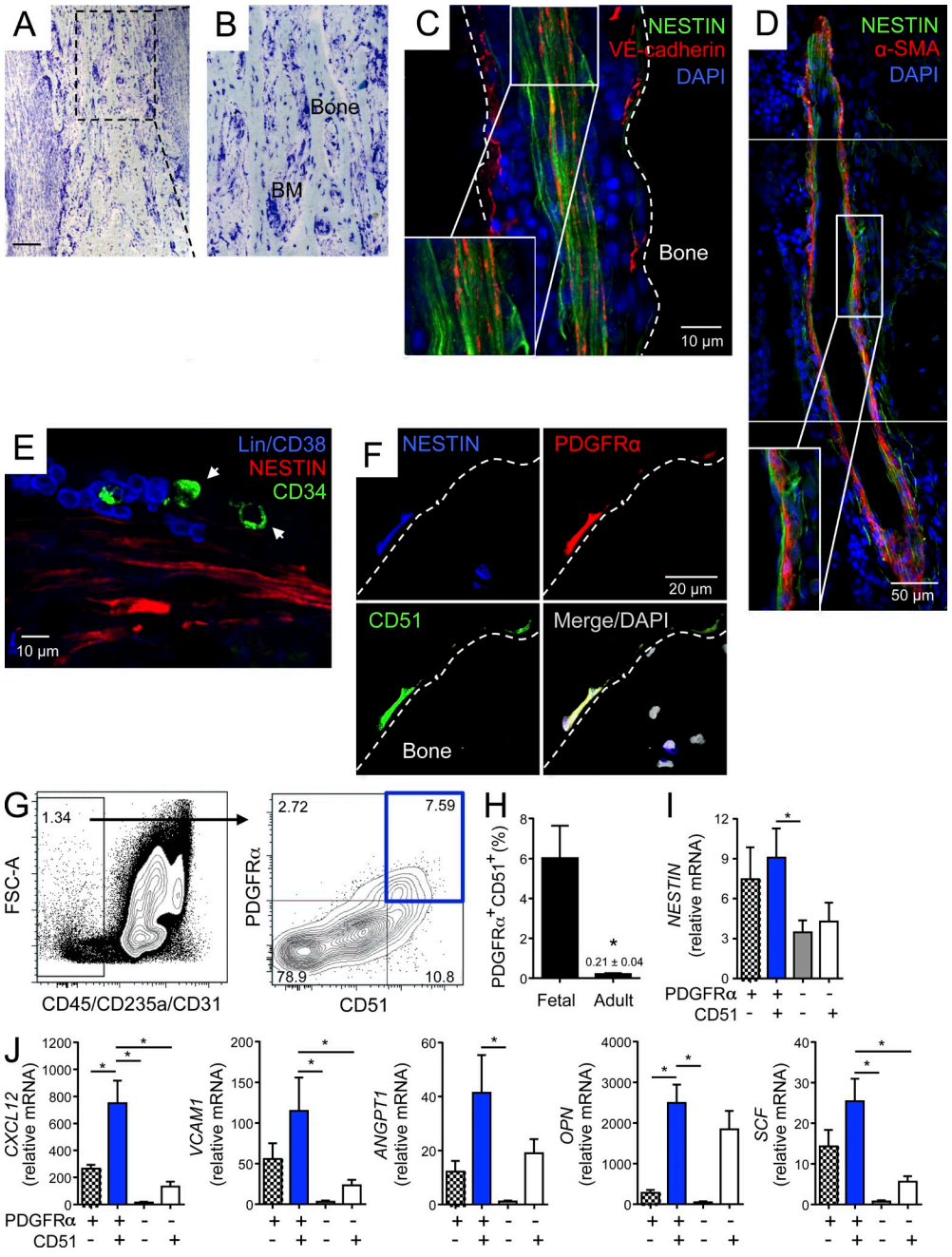

Figure 5. Perivascular Nestin⁺ cells are present in the human fetal BM and express PDGFRα⁺ CD51⁺ cell surface markers. (A and B) Representative Toluidine Blue–stained section of a 17-gw human fetal femur showing a general view of the diaphyseal area (A) and details of the human fetal BM histological organization (B). Magnification of the boxed area in A is shown in B. Bar, 555 µm. (C and D) Immunofluorescence staining for NESTIN⁺ cells and VE-cadherin⁺ endothelial cells (C) or α-smooth muscle actin⁺ (α-SMA; D) in arterial vessels extending from the diaphysis toward the metaphysis region. Cell nuclei were stained with DAPI. Magnified images of the boxed areas are depicted in the insets. (E) Immunostaining for hematopoietic lineage (Lin) and CD38, CD34, and NESTIN cells in the human fetal BM. Human Lin⁻ CD38⁻ CD34⁺ HSCs/progenitor cells are indicated by arrowheads. (F) Human fetal BM cells were stained for NESTIN, PDGFRα, and CD51 expression by triple-immunofluorescence staining. Cell nuclei were stained with DAPI. (C and F) White dashed lines demarcate compact bone areas. (G) Representative flow cytometric profile of freshly isolated stromal (CD45⁻ CD235a⁻ CD31⁻) PDGFRα⁺ CD51⁺ cells in human 19-gw fetal BM. (H) Comparison of the PDGFRα⁺ CD51⁺ cell frequency in the stromal population between fetal and adult BM. $n = 16$ fetal and $n = 6$ adult BM independent samples. (I and J) Stromal PDGFRα⁺ CD51⁺ cells were sorted from human fetal BM samples and *NESTIN* (I), and *CXCL12*, *VCAM1*, *ANGPT1*, *OPN*, and *SCF* mRNA levels were measured by real-time PCR (J). $n = 4$ independent experiments. *, $P < 0.05$; unpaired two-tailed Student's *t* test. All error bars indicate SEM.

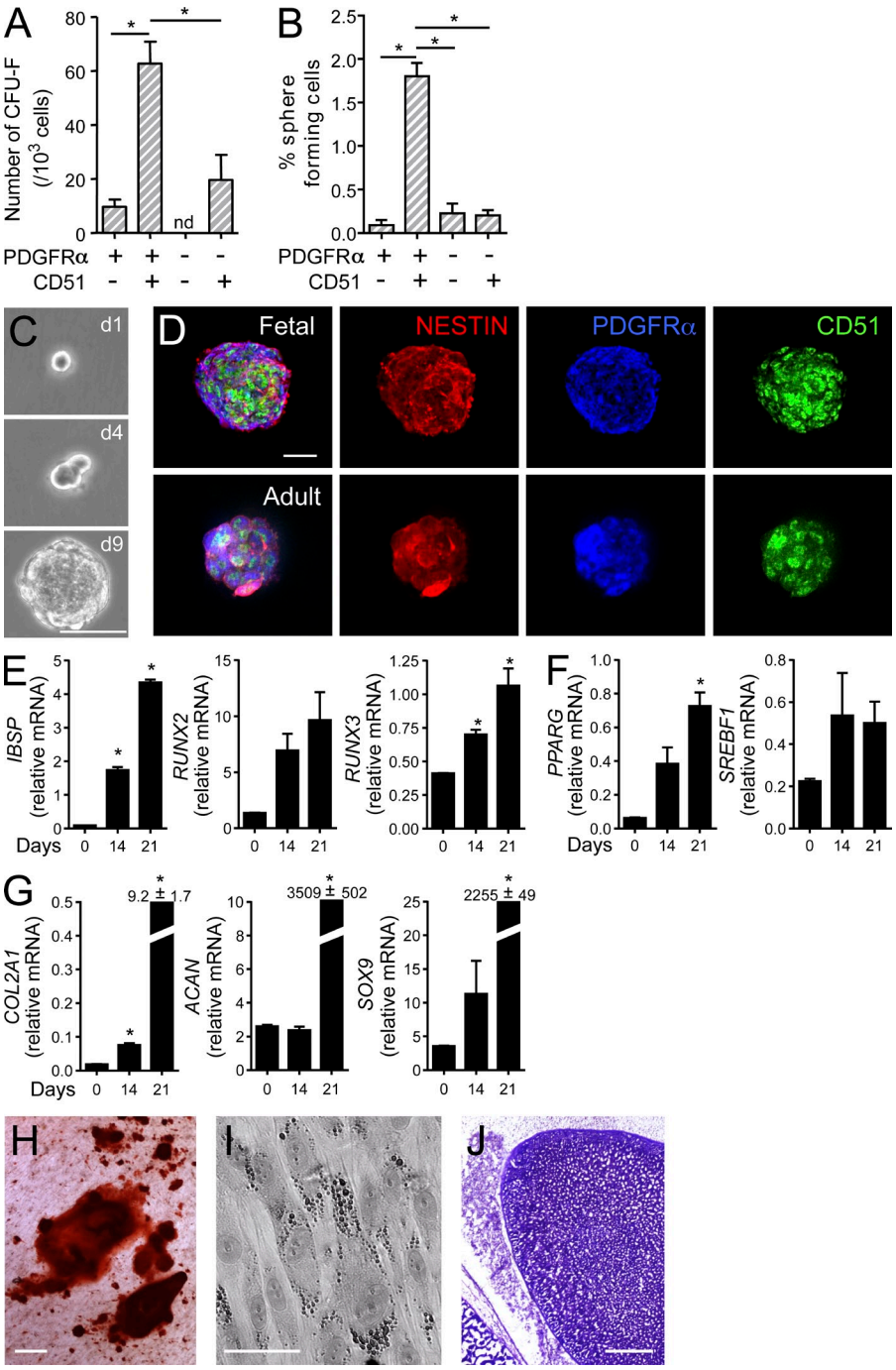

Figure 6. MSC activity of human fetal BM PDGFRα⁺ CD51⁺ cells. (A and B) Human fetal BM PDGFRα and CD51 populations were isolated and tested for CFU-F (A) and self-renewing clonal nonadherent sphere formation capacity (B). $n = 3$ independent sorting experiments; nd, not detectable. (C) Example of clonal sphere growth at days 1, 4, and 9. (D) Immunofluorescence analysis of fetal and adult human BM PDGFRα⁺ CD51⁺ clonal spheres in culture tested for NESTIN expression. (E–G) Multilineage differentiation capacity of human fetal PDGFRα⁺ CD51⁺ spheres was evaluated by gene expression analyses of osteoblastic (*IBSP*, *RUNX2*, and *RUNX3*; E), adipogenic (*PPARG* and *SREBF1*; F), and chondrogenic (*COL2A1*, *ACAN*, and *SOX9*; G) lineage differentiation genes during a 21-d period. $n = 3$. (H–J) Differentiated phenotype of human fetal PDGFRα⁺ CD51⁺ spheres was assessed using Alizarin Red S (osteogenic) staining (H), lipid vacuole accumulation (adipogenic; I), and Toluidine Blue (chondrogenic) staining (J). Bars: (C, D, and J) 50 µm; (H and I) 100 µm. *, $P < 0.05$; unpaired two-tailed Student's *t* test. All error bars indicate SEM.

analysis of the fractionation of total CD146⁺ population in PDGFRα⁺ CD51⁺ (green gate) and non–double-positive cells (black gate) also confirmed that PDGFRα⁺ CD51⁺ cells were an enriched fraction for HSC maintenance genes within the CD146⁺. In addition, we have also observed that within the CD146⁺ population, most of the sphere-forming capacity was within the PDGFRα⁺ CD51⁺ subset (Fig. 7 D). These results indicate that PDGFRα⁺ CD51⁺ are a small subset of the CD146⁺ population that markedly enriches for HSC niche and MSC activities in the human fetal BM.

HSC niche activity of human fetal PDGFRα⁺ CD51⁺ cells

To assess in vivo self-renewal, single clonal human PDGFRα⁺ CD51⁺ spheres were culture-expanded and transplanted in conjunction with hydroxyapatite/tricalcium phosphate (HA/TCP) carrier particles s.c. into immunodeficient mice. Before transplantation, culture-expanded cells homogeneously expressed PDGFRα and CD51. 8 wk after transplantation, foci of murine hematopoietic activity could be detected inside the graft (Fig. 8 A). Because PDGFRα and CD51 epitopes are sensitive to degradation as a result of the decalcification process,

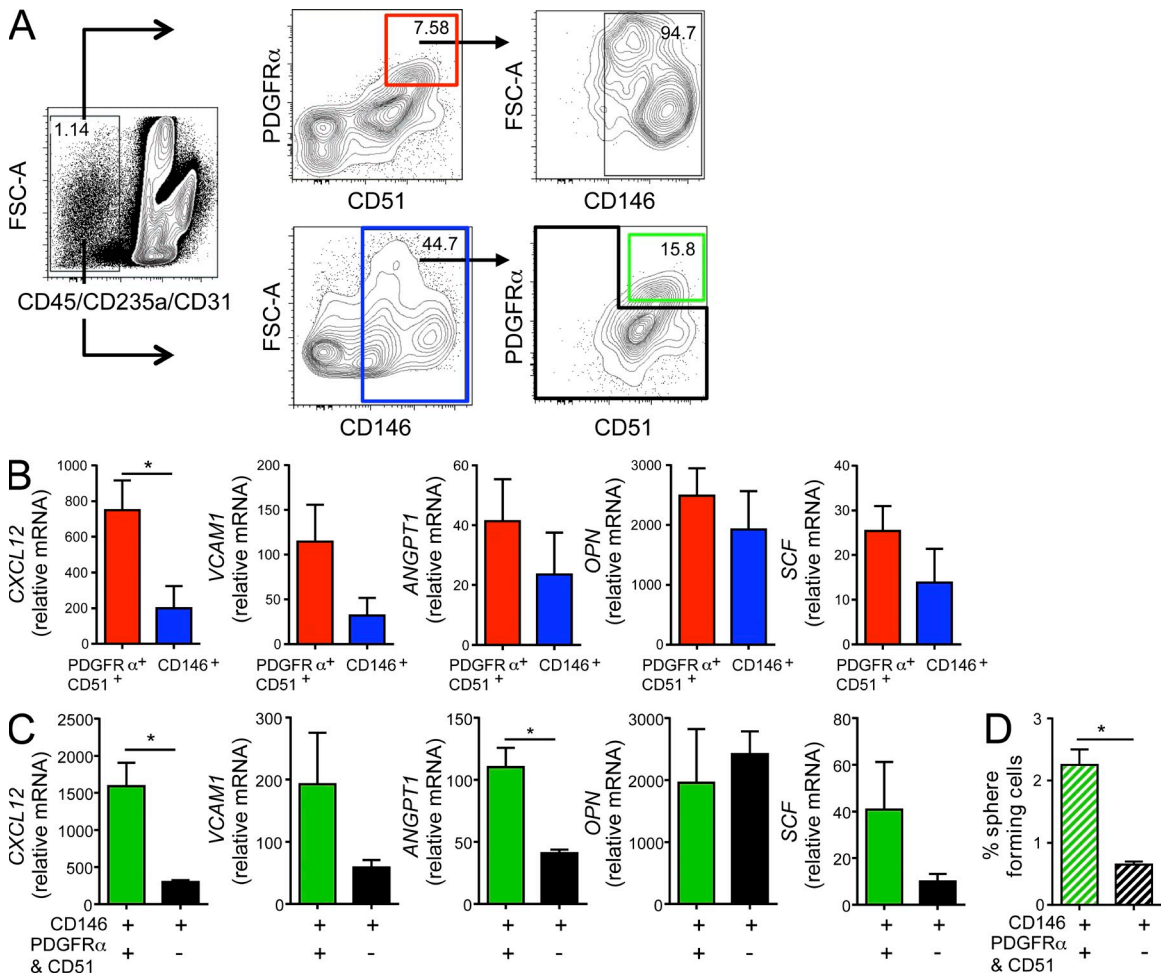

Figure 7. Human PDGFRα⁺ CD51⁺ cells represent a small subset of the CD146⁺ BM population enriched for HSC niche and MSC activities. (A) Human CD45⁻ CD235a⁻ CD31⁻ stromal fetal BM cells were analyzed for PDGFRα, CD51, and CD146 cell surface marker expression by flow cytometry. Numbers indicate the percentage of positive cells present in the indicated gates. Data are representative of six to nine independent analyses with comparable results. (B and C) Gene expression analysis of *CXCL12*, *VCAM1*, *ANGPT1*, *OPN*, and *SCF* was compared between stromal PDGFRα⁺ CD51⁺ (red gate) and CD146⁺ (blue gate) populations (B) and between PDGFRα and CD51 double-positive (green gate) and negative (black gate) fractions within CD146⁺ cells (C) by real-time PCR. (D) Capacity to form clonal nonadherent spheres in culture was compared between PDGFRα and CD51 double-positive (green) and negative (black) fractions within the stromal CD146⁺ population. $n = 3$ 15–18-gw human fetal BM samples. *, $P < 0.05$; unpaired two-tailed Student's *t* test. All error bars indicate SEM.

we evaluated the presence of MSCs in situ by staining for human-specific anti-NESTIN. Self-renewing Nestin⁺ cells were detected in the perivascular regions surrounding branching vessels containing murine Ter119⁺ red blood cells (Fig. 8, B–D). In addition, other constituents of the HSC stromal niche resembling the fetal BM microenvironment were also observed, including immature hyaline-like cartilage nodules, bone osteoid–like matrix containing osteoblast-like cells, and adipocytes (not depicted). Consistent with their self-renewal capacity, transplanted human PDGFRα⁺ CD51⁺ cells were capable of forming human secondary clonal spheres in culture (Fig. 8 E) that retained PDGFRα, CD51, and NESTIN expression (Fig. 8 F), as seen by immunofluorescence staining using human-specific anti-CD51 and anti-NESTIN antibodies. To further determine whether the ectopic grafts loaded with human PDGFRα⁺ CD51⁺ cells could provide a functional niche for circulating recipient HSCs to engraft, we verified by FACS analysis the presence of phenotypic HSCs and progenitor cells. To ensure that the hematopoietic cells inside the ossicles were not derived from the human transplanted BM stromal cells but recruited from the recipient mice, all analyzed cells were gated on mouse CD45⁺ cells using a species-specific antibody. The frequency of CD45⁺ cells in the PDGFRα⁺ CD51⁺ ectopic grafts tended to be higher than in the control grafts ($P = 0.104$). However, the frequency of phenotypic hematopoietic progenitors (CD41⁻ Lin⁻ Sca1⁺ c-Kit⁺) and HSCs (CD41⁻ Lin⁻ Sca1⁺ c-Kit⁺ CD48⁻ CD150⁺) in the PDGFRα⁺ CD51⁺ ectopic grafts was approximately eight- and sixfold higher in the PDGFRα⁺ CD51⁺ grafts than in the control group, respectively (Fig. 8 G). These results suggest that human PDGFRα⁺ CD51⁺ cells isolated from fetal BM are able to initiate ectopic HSC niche formation and recruit circulating HSCs and progenitors into the ectopic graft.

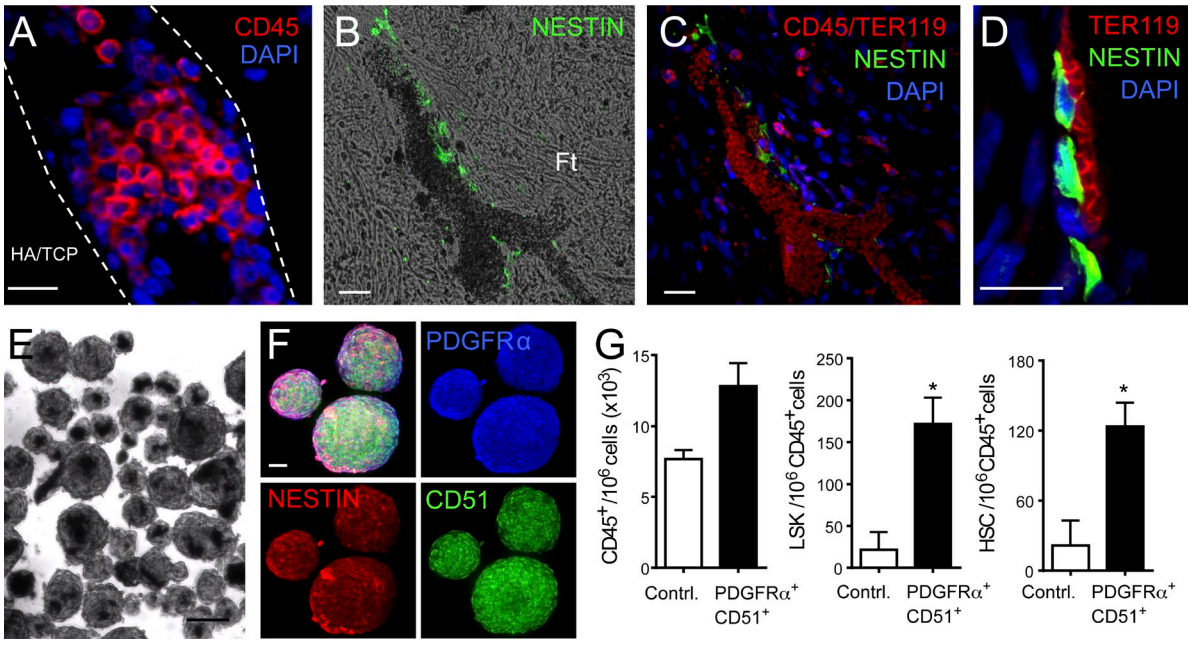

Figure 8. HSC niche activity in heterotopically transplanted human PDGFRα⁺ CD51⁺ stromal cells. (A) Immunofluorescence staining for CD45⁺ hematopoietic clusters inside the ectopic graft 8 wk after s.c. implantation in NSG mice. White dashed lines delineate HA/TCP carrier particles. (B–D) Immunofluorescence staining for NESTIN⁺ cells and murine Ter119⁺ erythroid cells inside branching sinusoids in the ectopic grafts. Cell nuclei were stained with DAPI. Ft, mesenchymal fibroblastic tissue. (E) Self-renewal capacity of PDGFRα⁺ CD51⁺ clonal spheres to form secondary spheres in culture was tested by plating dissociated transplanted human grafted cells collected 8 wk after implantation. (F) The human donor origin of secondary spheres was tested by immunofluorescence staining with PDGFRα and human species-specific CD51 and NESTIN antibodies. (G) Flow cytometry quantification of mouse CD45⁺ cells, CD45⁺ CD41⁻ Lin⁻ Sca-1⁺ c-Kit⁺ cells (LSK), and CD45⁺ CD41⁻ LSK CD48⁻ CD150⁺ HSCs recruited in PDGFRα⁺ CD51⁺ human ectopic grafts. Bars: (A–D) 20 µm; (E) 100 µm; (F) 50 µm. *, $P < 0.05$; unpaired two-tailed Student's *t* test. All error bars indicate SEM.

Human PDGFRα⁺ CD51⁺ mesenspheres expand HSPCs ex vivo

Because PDGFRα⁺ CD51⁺ cells exhibit HSC niche activity when transplanted in immunodeficient mice, we then assessed their capacity to maintain HSCs and progenitors ex vivo. To this end, we co-cultured nonadherent PDGFRα⁺ CD51⁺ mesenspheres with fetal human BM CD34⁺-enriched cells in serum-free media containing SCF, thrombopoietin (TPO), and Flt3 ligand (Flt3L). After 10 d, the number of hematopoietic cells (CD45⁺), multipotent progenitors (MPPs; CD45⁺ Lin⁻ CD34⁺ CD38⁻ CD90⁻ CD49f⁻), and HSC-enriched population (CD45⁺ Lin⁻ CD34⁺ CD38⁻ CD90⁺ CD49f⁺), as previously described (Notta et al., 2011), were determined by FACS (Fig. 9 A). We found that mesenspheres were able to expand HSC-enriched cell population by 11.2-fold after 10 d compared with the day 0 input (Fig. 9 B). In addition, HSC expansion was 2.4-fold greater using mesenspheres compared with media containing only hematopoietic growth factors (SCF, TPO, and Flt3L). We also observed that the number of hematopoietic cells (CD45⁺), MPPs, and CFUs in culture (CFU-Cs) per well were also significantly increased after co-culture with PDGFRα⁺ CD51⁺ mesenspheres during the same period of time (Fig. 9 B).

To validate the expansion of phenotypic HSPCs, we performed two functional assays. First we quantified the frequency of long-term culture-initiating cells (LTC-ICs) among Lin⁻ CD34⁺ cells. Using this strategy, we observed that the number of LTC-ICs was increased by twofold when CD34⁺ cells were cultured with mesenspheres in comparison with CD34⁺ cells cultured with cytokines only (Fig. 9 C). Second, we analyzed the engraftment ability of ex vivo–expanded HSCs and progenitors. We found that mesensphere-expanded fetal BM CD34⁺ cells led to a significant increase in the proportion of engrafted NSG mice 8 wk after transplantation (80% vs. 9%; $P < 0.05$, Fisher's exact test; Fig. 9 D). In contrast, there was a nonsignificant trend of enhanced engraftment in the group transplanted with cells cultured with cytokines only. Furthermore, mesensphere-expanded cells proved to have multilineage potential as they were able to differentiate along the myeloid and lymphoid lineages (Fig. 9 E). Collectively, these data demonstrate that PDGFRα⁺ CD51⁺ mesenspheres can efficiently expand a population enriched in HSPCs capable of multilineage engraftment.

HSPC expansion by PDGFRα⁺ CD51⁺ mesenspheres is contact independent

In the co-culture system, we observed that CD34⁺ cells tend to aggregate around the PDGFRα⁺ CD51⁺ mesenspheres (Fig. 10 A), raising the question of whether or not direct contact with the mesenspheres is necessary for the HSC/progenitor expansion. We therefore plated PDGFRα⁺ CD51⁺ mesenspheres either directly with CD34⁺ cells or in the upper chamber of a transwell unit with 0.4-µm pore polycarbonate membrane

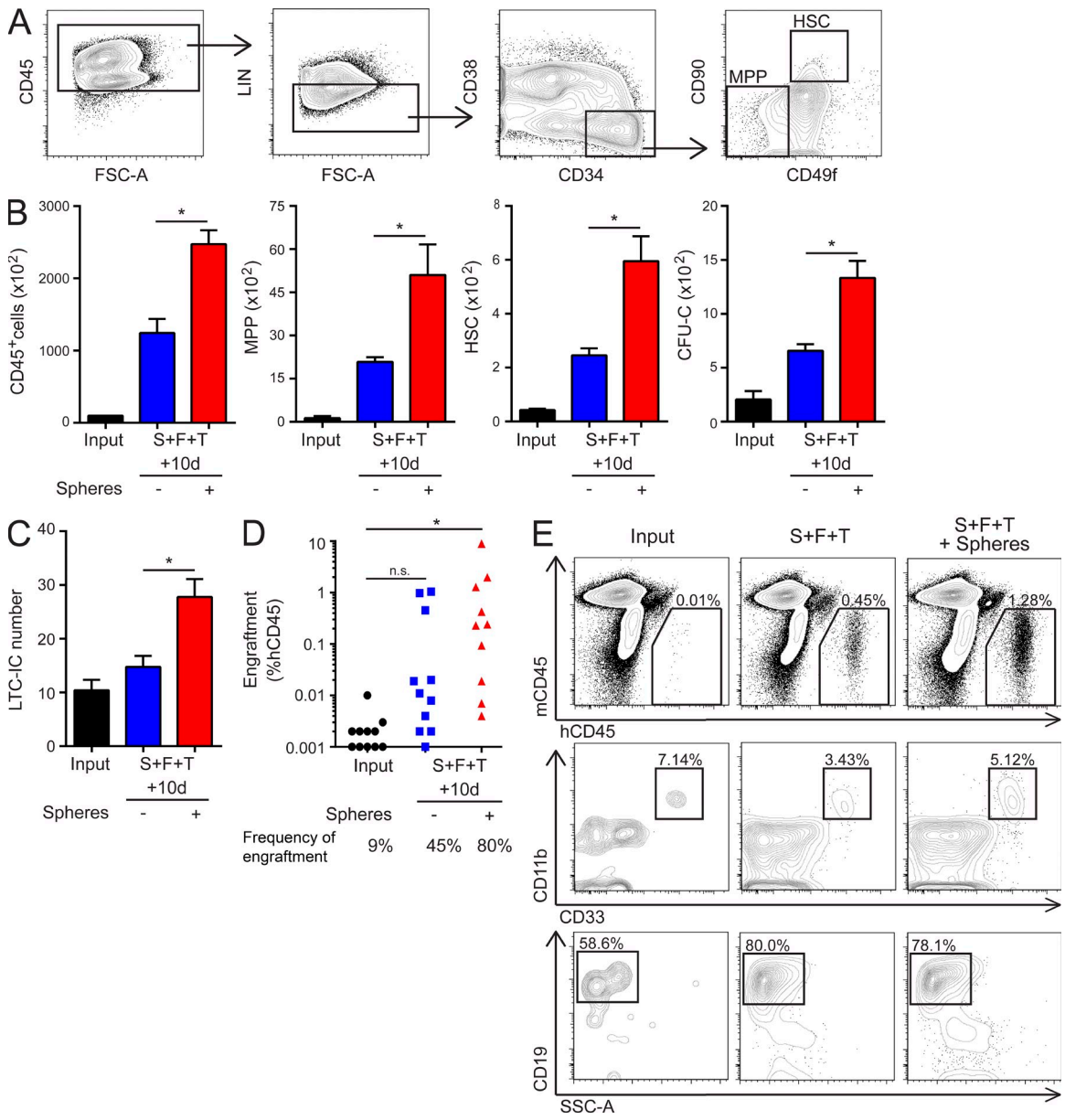

Figure 9. Fetal PDGFRα⁺ CD51⁺ mesenspheres expand HSPCs ex vivo. (A) Gating strategy used to analyze hematopoietic populations by flow cytometry. (B) CD34⁺ cells were co-cultured with PDGFRα⁺ CD51⁺ mesenspheres in serum-free media containing SCF, Flt3L, and TPO. CD45⁺ cells, MPPs, and HSC-enriched population were quantified by flow cytometry after 10 d. Cells were also scored for CFU-C activity. $n = 3$. (C) Long-term HSCs were quantified from the input Lin⁻ CD34⁺ population or after 10 d of co-culture with or without mesenspheres using LTC-IC assay. $n = 3$. *, $P < 0.05$; unpaired two-tailed Student's t test. All error bars indicate SEM. (D) 2×10^4 input CD34⁺ cells or a final culture equivalent to 2×10^4 CD34⁺ starting cells cultured with or without mesenspheres were transplanted into NSG mice, and human BM engraftment was evaluated 8 wk after transplantation. n = 10–11 mice per group. *, $P < 0.05$; Fisher's exact test; n.s., not significant. (E) Multilineage human hematopoietic engraftment was evaluated by detection of myeloid (CD11b and CD33) and lymphoid (CD19) markers. Representative flow cytometry plots of BM cells from each experimental condition are shown.

to prevent direct contact with CD34⁺ cells. Unexpectedly, we observed that direct contact between mesenspheres and CD34⁺ cells was not required for the expansion of CD45⁺ cells, MPPs, and HSC-enriched population (Fig. 10 B), suggesting that the secretion of soluble factors rather than membrane-bound factors by PDGFRα⁺ CD51⁺ mesenspheres accounts for their capacity to expand an HSC-enriched population. In an effort to quantify the capacity of PDGFRα⁺ CD51⁺ mesenspheres to expand HSCs, we then monitored cell expansion in function of the number of mesenspheres per well. Although we observed a positive correlation between the number of spheres and CD45⁺ cells, the population enriched in HSC activity seems to be more sensitive to sphere numbers (Fig. 10 C). A minimum of 15–25 spheres/well was required to significantly

promote HSC expansion, and in contrast, plating >25 mesenspheres/well negatively impacted the expansion of HSC-enriched population (Fig. 10 C). These results suggest that a very specific dosage of the factors secreted by PDGFRα$^+$ CD51$^+$ mesenspheres is essential to expand HSPCs.

Human PDGFRα$^+$ CD51$^+$ mesenspheres express SCF and rescue HSPC expansion in the absence of SCF

To gain some insight into the factors secreted by PDGFRα$^+$ CD51$^+$ mesenspheres mediating their capacity to expand HSPCs, we cultured CD34$^+$ cells with or without mesenspheres in media containing different combinations of cytokines. When SCF was absent from the culture media, the HSC-enriched population was significantly reduced. In these culture conditions, the presence of the PDGFRα$^+$ CD51$^+$ mesenspheres rescued HSPC expansion, yielding a 36- and 7.5-fold expansion, as compared with control media without mesenspheres and day 0 input, respectively (Fig. 10 D). In the absence of Flt3L or TPO, PDGFRα$^+$ CD51$^+$ mesenspheres also rescued HSC expansion, but the effect was not as marked. Indeed, PDGFRα$^+$ CD51$^+$ mesenspheres generated a 3.7- and 9.4-fold expansion in the absence of Flt3L and TPO, respectively, in comparison with media without spheres (Fig. 10 D). The expansion of MPPs and total CD45$^+$ cells was also rescued by PDGFRα$^+$ CD51$^+$ mesenspheres in all culture conditions. Furthermore, gene expression analyses revealed that PDGFRα$^+$ CD51$^+$ mesenspheres expressed high levels of *SCF* compared with total BM, whereas levels of *Flt3L* and *TPO* did not differ significantly (Fig. 10 E). Immunofluorescence analyses showed that PDGFRα$^+$ CD51$^+$ mesenspheres homogeneously expressed both NESTIN and SCF (Fig. 10 F). Thus, these data suggest that Nestin$^+$ PDGFRα$^+$ CD51$^+$ mesensphere-derived SCF is likely to play an important role in HSPC maintenance.

DISCUSSION

Although near homogeneous populations of HSCs and progenitors have been extensively isolated and characterized, the identity and role of the stromal cells regulating hematopoiesis remain largely undefined. Progress has been hampered by the limited availability of freshly isolated tissues and the paucity of selective stromal markers and genetic tools. Common methods to isolate human MSCs have widely relied on plastic adherence and in vitro expansion of adherent cells, which invariably lead to heterogeneous stromal populations whose biological and immunophenotypic properties are modulated in culture (Sacchetti et al., 2007; Delorme et al., 2008; Tanabe et al., 2008; Liu et al., 2012). Here, we have used Nes-*Gfp* transgenic mice that mark a highly enriched fraction of MSCs that form the HSC niche (Méndez-Ferrer et al., 2010) to identify an equivalent in situ population defined by PDGFRα$^+$ CD51$^+$ CD45$^-$ CD31$^-$ CD235a$^-$ (or Ter119$^-$ in mice) representing a subset of Nestin$^+$ cells that can be isolated prospectively in both mouse and human BM.

Although our previous study has suggested that the two stem cell types of the BM formed a single niche, only a small fraction of Nestin$^+$ cells exhibits MSC activity by mesensphere or CFU-F assays (Méndez-Ferrer et al., 2010), likely because of the combination of Nestin$^+$ cell heterogeneity and harsh isolation protocols that may have altered cell viability. The fact that the frequency of Nestin$^+$ cells (0.03–0.08%) in mouse BM is higher than that of HSCs left the possibility that MSC activity and HSC maintenance properties could be conferred by distinct cells. The present experiments have given more insight in this question as PDGFRα$^+$ CD51$^+$ stromal cells marked a subset (~60%) of Nestin$^+$ cells that enriched similarly for both HSC niche and MSC activities compared with the remaining Nestin$^+$ cells. These results lend further support to the idea that these two activities may co-segregate in the BM.

Our results show that PDGFRα, an early development marker of a transient wave of MSC progenitors derived from neuroepithelial and neural crest lineages (Takashima et al., 2007), is a major surface marker for Nestin$^+$ MSCs. Because neural crest stem cell–derived spheres also express Nestin (Nagoshi et al., 2008), both markers may overlap during early development. Our data indeed predict a significant overlap between Nestin$^+$ cells and a population of CD45$^-$ Tie-2$^-$ CD51$^+$ CD105$^+$ CD90$^-$ cells isolated from embryonic day 15.5 mouse fetal bones capable of generating heterotopic BM niche in a transplantation model (Chan et al., 2009). Although PDGFRα was recently used to isolate CD45$^-$ Ter119$^-$ PαS cells from the adult mouse bone that enriched for CFU-F activity and differentiation capability into mesenchymal lineages (Morikawa et al., 2009), our study suggests that in the BM, Nestin$^+$ and PαS cells are distinct cell populations. The fact that a higher proportion of Nestin$^+$ cells express Sca-1 in bone raises interesting questions about functional differences of bone- versus BM-derived MSCs that should be investigated in the future.

A major advance of the current study is the identification a population similar to Nestin$^+$ perivascular cells in the human BM, which lie in close contact with human HSCs/progenitor cells. In the human fetal BM, PDGFRα and CD51 mark a subset of stromal cells expressing Nestin that is highly enriched in CFU-F activity. Like its mouse counterpart, freshly sorted human stromal PDGFRα$^+$ CD51$^+$ cells also express high levels of HSC maintenance genes and efficiently form clonal multipotent self-renewing mesenspheres. Importantly, these cells could heterotopically reconstitute a BM niche populated by recruited HSPCs, and containing a subset of self-renewing perivascular cells that retained NESTIN expression.

A previous study has shown that human CD146$^+$ BM cells comprised osteoprogenitors capable of generating hematopoiesis in heterotopic bones (Sacchetti et al., 2007). Although our results indicate that CD146 is not expressed on murine Nestin$^+$ cells, a genome-wide expression profile of these cells was closest to that of human CD146$^+$ BM cells (Méndez-Ferrer et al., 2010), suggesting that human CD146 may mark a stromal cell similar to murine Nestin$^+$ cells. Indeed, our results in the human system indicate that PDGFRα$^+$ CD51$^+$ cells comprise a restricted subset of CD146$^+$ stromal cells further enriched for HSC niche and MSC activities in the fetal human BM.

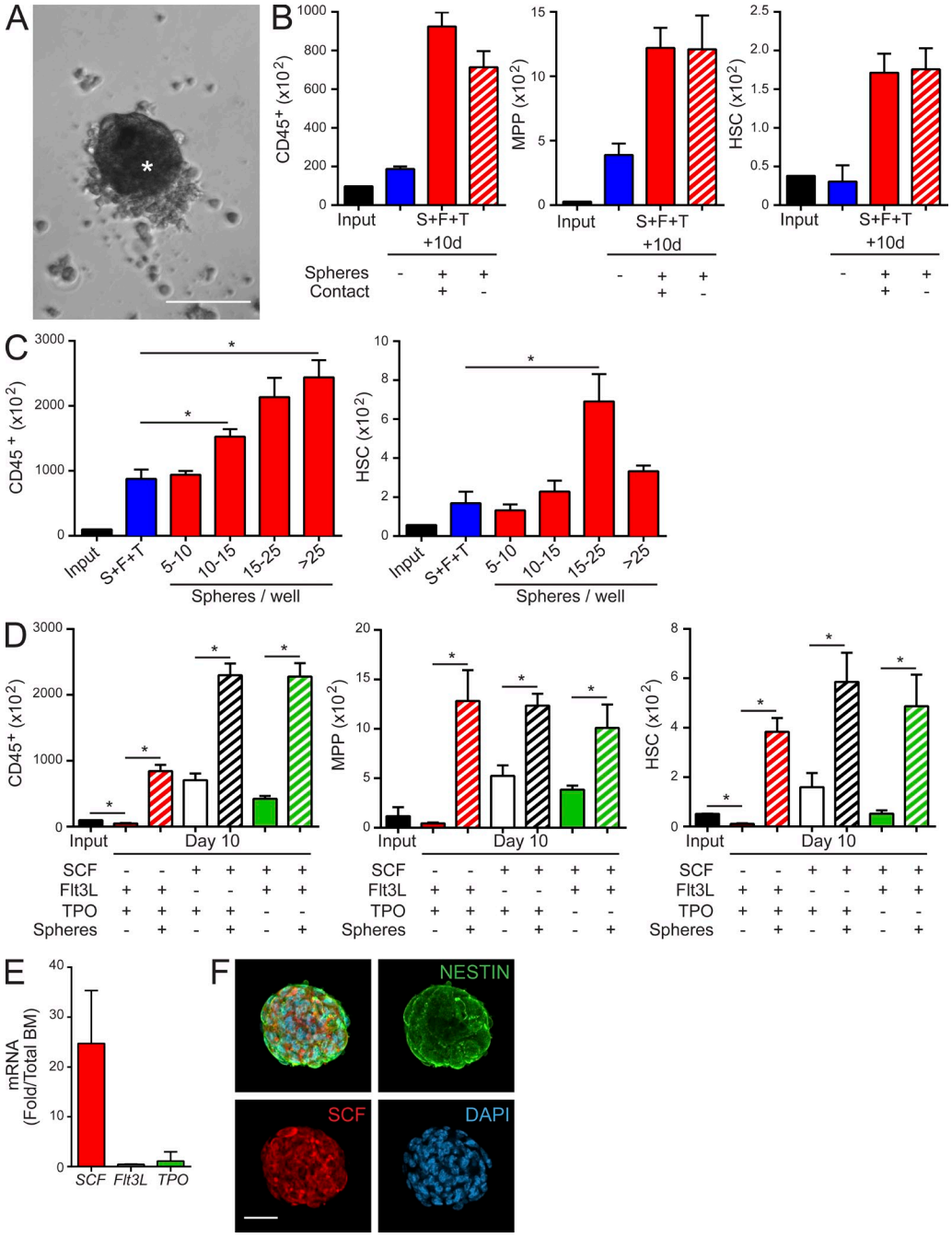

Figure 10. Fetal PDGFRα+ CD51+ mesenspheres expand HSPCs in a contact-independent manner and can compensate for the absence of SCF. (A) Representative picture showing CD34+ cell aggregation around PDGFRα+ CD51+ mesenspheres in co-culture assays. The asterisk marks a mesensphere. (B) PDGFRα+ CD51+ mesenspheres were plated either directly with CD34+ cells in the lower chamber of a 96-transwell unit or in the upper chamber to prevent direct contact. $n = 3$. (C) PDGFRα+ CD51+ mesenspheres were plated at different densities with a constant number of CD34+ cells. CD45+ and HSC-enriched populations were quantified 10 d later by flow cytometry. $n = 3$. (D) CD34+ cells were co-cultured with PDGFRα+ CD51+ mesenspheres in serum-free media containing Flt3L + TPO, SCF + TPO, or SCF + Flt3L. After 10 d, CD45+, MPPs, and HSC-enriched populations were detected by flow cytometry. $n = 3$. (E) Real-time PCR expression analysis of *SCF*, *Flt3L*, and *TPO* in PDGFRα+ CD51+ mesenspheres. Fold increase over total BM is shown. $n = 3$. (F) Immunofluorescence analyses of a representative human PDGFRα+ CD51+ mesensphere testing the coexpression of NESTIN and SCF. Bars, 50 µm. *, $P < 0.05$; unpaired two-tailed Student's *t* test. All error bars indicate SEM.

Ex vivo human HSC expansion still represents a challenge in part because of our limited knowledge on the in vivo HSC niche constituents and factors secreted by these cells. Our study shows that PDGFRα+ CD51+ mesenspheres expand a population containing phenotypically defined CD45+ Lin− CD34+ CD38− CD90+ CD49f+ long-term HSCs (Notta et al., 2011).

Although this set of markers was not validated after prolonged culture, we found that expansion of the CD45$^+$ Lin$^-$ CD34$^+$ CD38$^-$ CD90$^+$ CD49f$^+$ cell population correlated with both LTC-IC expansion and increased engraftment in NSG mice. Our study thus provides a novel three-dimensional co-culture system using PDGFRα$^+$ CD51$^+$ mesenspheres that will likely prove to be a useful platform to identify niche components critical for HSC ex vivo maintenance and expansion.

We have explored herein the role of SCF because a recent study has suggested that it was produced by endothelial and LepR$^+$ perivascular cells that were distinct from Nestin$^+$ cells in mouse BM (Ding et al., 2012). However, Nestin$^+$ MSCs also express high levels of SCF (Méndez-Ferrer et al., 2010), and our results indeed indicate that LepR$^+$ cells largely overlap with Nes-GFP$^+$ cells and that the PDGFRα$^+$ CD51$^+$ fraction within the Nestin$^+$ population also contains most of the stromal LepR$^+$ cells. In human BM, our analyses show that PDGFRα$^+$ CD51$^+$ mesenspheres that uniformly express NESTIN and SCF have a direct impact on the ex vivo expansion of HSCs/progenitors and can rescue HSC maintenance in the absence of exogenous SCF. Altogether, these data strongly suggest that Nestin$^+$ cells may represent an essential source of SCF in the human BM.

In summary, our results demonstrate the existence of a self-renewing, multipotent population of Nestin$^+$ MSCs as an important constituent of the human fetal HSC niche. Thus, this study provides the groundwork for isolation of highly purified populations of MSCs that will shed important insight on the molecular mechanisms mediating HSC maintenance and expansion.

MATERIALS AND METHODS

Mouse strains. All murine experiments were performed using adult 8–12-wk-old animals. All mice were housed in specific pathogen–free facilities at the Albert Einstein College of Medicine (Einstein) animal facility, and all of the experimental procedures were approved by the Animal Care and Use Committee of Einstein. C57BL/6 and C57BL/6 Ly5.2 (CD45.1) mice were purchased from the National Cancer Institute (Frederick Cancer Research Center). B6.129-*Lepr*$^{tm2(cre)Rck}$/J (LepR-*cre*) and B6.Cg-*Gt(ROSA)26Sor*$^{tm14(CAG-tdTomato)Hze}$/J (LSL-td*Tomato*) mice were purchased from The Jackson Laboratory. Nes-*Gfp* transgenic mice (Mignone et al., 2004) and *NOD-scid Il2rg*$^{-/-}$ (NSG) immunocompromised mice were bred and used at Einstein.

Cell isolation. BM primary cells were isolated as previously described (Méndez-Ferrer et al., 2010) with minor modifications. In brief, femora, tibia, and humeri BM were gently flushed in L-15 FACS buffer (Méndez-Ferrer et al., 2010) and after erythrocyte lysis, digested with 1 mg/ml collagenase IV (Sigma-Aldrich) in HBSS (Gibco) with 10% FBS (STEMCELL Technologies) for 30 min at 37°C. For flow cytometry sorting, cells were enriched by immunomagnetic depletion using anti-CD45 magnetic beads (Miltenyi Biotec) according to the manufacturer's recommendations. Cells were sorted on a FACSAria (BD) to >95% purity. Human fetal BM samples, between 13 and 20 gw, were obtained from the Einstein Human Fetal Tissue Repository by protocols approved by the Institutional Review Board. Human fresh adult BM samples were commercially obtained from Lonza.

Flow cytometry. Fluorochrome-conjugated or biotinylated mAbs specific to mouse CD45 (clone 30-F11), CD45.1 (clone A20), Ter119 (clone Ter-119), PDGFRα (clone APA5), CD51 (clone RMV-7), CD44 (clone IM7), CD130 (clone KGP130), c-Kit (clone 2B8), CD135 (clone A2F10), CD90 (clone 53-2.1), CD34 (clone RAM34), CD166 (clone eBioALC48), Sca-1 (clone D7), CD41 (clone MWReg30), CD133 (clone 13A4), CD11b (clone M1/70), CD150 (clone TC15-12F12.2), CD61 (clone 2C9.G3), hematopoietic lineage cocktail, and corresponding isotype controls were purchased from eBioscience. P75 (clone 2E3) was purchased from Abcam. CD10 (clone SN5c/L4-1A1) was purchased from Santa Cruz Biotechnology, Inc. CD31 (clone MEC13.3), CD105 (clone MJ7/18), and CD48 (clone HM48-1) were from purchased from BioLegend, whereas CD29 (clone KMI6) and CD146 (clone ME-9F1) were purchased from BD. Ng2 rabbit polyclonal was obtained from EMD Millipore. Secondary antibodies Alexa Fluor 633 goat anti–rabbit IgG, Alexa Fluor 633 goat anti–mouse IgG, and Alexa Fluor 633 goat anti–rat IgG were obtained from Molecular Probes. Fluorochrome-conjugated mAbs specific to human CD45 (clone 2D1), CD235a (clone HIR2), CD31 (clone WM59), hematopoietic lineage cocktail, CD38 (clone HB7), CD49f (clone eBioGoH3), CD90 (clone eBio5E10), CD34 (clone 4H11), CD11b (clone ICRF44), CD33 (clone WM-53), and CD19 (clone HIB19) were obtained from eBioscience. PDGFRα (clone αR1) and CD146 (clone PIH12) were purchased from BD, and finally CD51 (clone NKI-M9) was purchased from BioLegend. Nes-GFP–positive staining was gated in reference to cells from wild-type mice without the GFP transgene, and positive specific antibody labeling was gated in reference to corresponding isotype control or fluorescence-minus-one (FMO) corresponding sample. Multiparameter analyses of stained cell suspensions were performed on an LSRII (BD) and analyzed with FlowJo software (Tree Star). DAPI$^-$ single cells were evaluated for all of the analyses.

Cell culture and differentiation. For clonal sphere formation, cells were plated at clonal density (<500 cells/cm^2) or by single cell sorting into ultra-low adherent plates as previously described (Méndez-Ferrer et al., 2010). Cells were kept at 37°C with 5% CO_2 in a water-jacketed incubator and left untouched for 1 wk to prevent cell aggregation. One-half medium changes were performed weekly. All spheres in a given well were counted at day 9, and results are expressed as a percentage of plated cells.

For osteogenic, adipogenic, and chondrogenic differentiation, mouse or human PDGFRα$^+$ CD51$^+$ cells were treated with StemXVivo Osteogenic, Adipogenic, or Chondrogenic mouse- or human-specific differentiation media, according to the manufacturer's instructions (R&D Systems). All cultures were maintained with 5% CO_2 in a water-jacketed incubator at 37°C. At specific time points, cells were collected for RNA or cytochemistry analysis. Osteogenic differentiation indicated by mineralization of extracellular matrix and calcium deposits was revealed by Alizarin Red S staining. Cells were fixed with 4% paraformaldehyde (PFA) for 30 min. After rinsing in distilled water, cells were stained with 40 mM Alizarin Red S (Sigma-Aldrich) solution at pH 4.2, rinsed in distilled water, and washed in Tris-buffered saline for 15 min to remove nonspecific staining. Adipocytes were identified by the typical production of lipid droplets. Chondrocytes were revealed by Toluidine Blue staining, which detects the synthesis of glycosaminoglycans. Cells were fixed with 4% PFA for 60 min, embedded in paraffin, and sectioned. Sections were incubated with 0.5% Toluidine Blue (Sigma-Aldrich) in distilled water for 15 min. To remove nonspecific staining, sections were rinsed thrice with running water (5 min each).

CFU-F assay. 1–3 × 10^3 mouse sorted cells were seeded per well in a 12-well adherent tissue culture plate using phenol red–free α-MEM (Gibco) supplemented with 20% FBS (Hyclone), 10% MesenCult stimulatory supplement (STEMCELL Technologies), and 0.5% penicillin-streptomycin. One half of the media was replaced after 7 d and at day 14 cells were stained with Giemsa staining solution (EMD Chemicals). Human fetal BM cells were plated at 0.5–1 × 10^3 cells/well into 6-well adherent tissue culture plates using phenol red–free α-MEM with 20% FBS (STEMCELL Technologies) and 0.5% penicillin-streptomycin. One half of the media was replaced after 5 d, and at day 10 cells were stained and adherent colonies counted.

RNA isolation and quantitative real-time PCR. Sorted or cultured cells were collected in lysis buffer, and RNA isolation was performed using the Dynabeads mRNA DIRECT Micro kit (Invitrogen). Reverse transcription was performed using the RNA to cDNA EcoDry Premix system (Takara Bio Inc.) according to the manufacturer's recommendations. Quantitative real-time PCR was performed as previously described (Méndez-Ferrer et al., 2010).

The relative mRNA abundance was calculated using the ΔCt method and multiplied by 100. Gene expression data were normalized to *Gapdh*. Human and mouse primer sequences are included in Table S1.

Immunofluorescence staining. Human fetal bones and HA/TCP grafts were fixed with 4% PFA for 2 h at 4°C, partially decalcified with 0.25 M EDTA for 2–3 d, and cryoprotected with 15–30% sucrose. Samples were then processed as described previously (Kawamoto, 2003) and immunostained using standard technique. Mesenspheres, collagen, and gelfoam grafts were also processed as described above without the decalcification step and using Superfrost Plus slides (Thermo Fisher Scientific). The following antibodies were used as primary: Alexa Fluor 488 anti-GFP (Molecular Probes), anti–mouse CD45-PE (clone 30-F11; eBioscience), anti–mouse Ter119-PE (clone Ter119; eBioscience), anti–human NESTIN (clone 196908 [R&D Systems] and N5413 [Sigma-Aldrich]), anti–human PDGFRα (clone C-20; Santa Cruz Biotechnology, Inc.), anti–human CD51-FITC (clone NKI-M9; BioLegend), anti–human VE-cadherin (clone 16B1; eBioscience), anti–human α-SMA–Cy3 (clone 1A4; Sigma-Aldrich), anti–human lineage-APC cocktail (eBioscience), anti–human CD38 (clone HIT2; eBioscience), and anti–human CD34-FITC (clone AC136; Miltenyi Biotec). The secondary antibodies used were Alexa Fluor 633 goat anti–mouse IgG, Alexa Fluor 568 goat anti–rabbit IgG, and Alexa Fluor 488 goat anti–mouse IgG (Molecular Probes). For nuclear staining, samples were treated with DAPI (Sigma-Aldrich). Images were captured using an Axio Examiner D1 confocal microscope (Carl Zeiss), and images were processed using the SlideBook software (Intelligent Imaging Innovations). We processed human fetal bones for Toluidine Blue staining as described previously (Kawamoto, 2003).

In vivo transplantation. For renal capsule collagen graft, five thousand freshly sorted cells or single spheres were gently resuspended in 15 µl of a collagen (BD) mixed with 2% of 1N NaOH and 10% of 10× PBS. The cell/collagen mix was then gently deposited into a 6-well plate and incubated at 37°C for 30 min to allow the collagen to solidify. Collagen grafts were then transplanted under the renal capsule of 8–12-wk-old anaesthetized mice. After 8 wk, kidneys/grafts were collected and processed for immunofluorescence and FACS analyses.

For s.c. gelfoam graft, transplantations were performed as previously described (Bianco et al., 2006) with minor alterations. Five thousand freshly sorted cells or single spheres were gently resuspended in 50 µl of sphere media. 5-mm^3 cubes of sterile collagen sponges (Gelfoam; Pfizer) were hydrated into sphere media and then squeezed to remove air bubbles and allow the sponge to regain its size. Just before transplantation, sponges were blotted between two pieces of sterile filter paper and placed in contact with the cell mixture at 37°C for 90 min. As the sponges expanded, they incorporated the cells. Gelfoam grafts were then implanted s.c. under the dorsal skin of 8–12 wk-old anaesthetized recipient animals. After 8 wk, gelfoam grafts were collected and processed for immunofluorescence analysis.

For s.c. HA/TCP graft, transplantation of human fetal cells was performed as described previously (Kuznetsov et al., 1997) with minor modifications. 5×10^5 cells derived from a clonally expanded sphere or 5×10^5 nonclonally expanded cells resuspended into sphere media were allowed to attach the HA/TCP powder (Ceraform; Teknimed SA) by slow rotation at 37°C. After 60 min, cell mixture was spun and media replaced by collagen (BD) mixed with 2% of 1N NaOH and 10% of 10× PBS. Grafts were incubated for another 30 min at 37°C and transplanted s.c. into 8–12-wk-old anaesthetized NSG recipient mice. After 8 wk, HA/TCP grafts were collected and processed for immunofluorescence and FACS analysis as described previously (Kuznetsov et al., 1997).

Isolation of human $CD34^+$ cells and co-culture with $PDGFR\alpha^+$ $CD51^+$ mesenspheres. Human fetal BM $CD34^+$ cells were isolated using anti–human $CD34^+$ magnetic microbeads (Miltenyi Biotec). 10^4 $CD34^+$ cells were co-cultured with or without $PDGFR\alpha^+$ $CD51^+$ mesenspheres in serum-free media (StemSpan; STEMCELL Technologies) supplemented with 25 ng/ml of recombinant human SCF, 12.5 ng/ml TPO, and 25 ng/ml Flt3L (R&D Systems) for 10 d at 37°C. $PDGFR\alpha^+$ $CD51^+$ mesenspheres were either plated directly with $CD34^+$ cells in a 96-well ultra-low attachment surface plate or in the upper chamber of a transwell unit with 0.4-µm pore polycarbonate membrane (Corning). 10 d after co-culture, cells were either FACS analyzed or plated in methylcellulose to score CFU-Cs (MethoCult Classical; STEMCELL Technologies). HSCs and MPP-enriched populations were analyzed as previously described (Notta et al., 2011).

LTC-IC assay. Human $CD34^+$ cells uncultured or cultured with cytokines for 10 d in the presence or absence of mesenspheres were plated at limiting dilution on human irradiated stroma in MyeloCult media H5100 (STEMCELL Technologies) containing 10^{-3} M hydrocortisone with weekly half-media changes. After 5 wk, the presence of LTC-ICs was scored based on CFU-Cs 2 wk after plating in MethoCult H4435 (STEMCELL Technologies). LTC-IC frequency was calculated by applying Poisson statistics using Limiting Dilution Analysis software (L-CALC; STEMCELL Technologies).

Transplantation into NSG mice. 2×10^4 fresh human $CD34^+$ cells or a final culture equivalent to 2×10^4 $CD34^+$ input cells cultured with or without mesenspheres were transplanted via the retroorbital route in NSG mice. NSG mice were sublethally irradiated (200 cGy) at least 4 h before transplantation. BM engraftment was analyzed 8 wk after transplantation by FACS. Mice were scored as engrafted when transplanted human cells reconstituted both myeloid and lymphoid lineages. Significance was calculated according to the Fisher's exact test.

Online supplemental material. Tables S1 shows primer sequences used for mouse and human quantitative real-time PCR analyses. Online supplemental material is available at http://www.jem.org/cgi/content/full/jem.20122252/DC1.

We would like to acknowledge Colette Prophete, Neepa Dholakia, and Matthew A. Huggins for technical assistance, Drs. Simón Méndez-Ferrer and Daniel Lucas for helpful suggestions, the Einstein Flow Cytometry Core Facility and the Human Stem Cell FACS Facility for expert cell sorting, the Stem Cell Institute Xenotransplantation Core for performing xenotransplantation experiments, and the Einstein Human Fetal Tissue Repository for providing human samples.

This work was supported by R01 grants from the National Institutes of Health (DK056638, HL097819, HL097700 to P.S. Frenette).

The authors have no conflicting financial interests.

Submitted: 5 October 2012
Accepted: 13 May 2013

REFERENCES

Arai, F., A. Hirao, M. Ohmura, H. Sato, S. Matsuoka, K. Takubo, K. Ito, G.Y. Koh, and T. Suda. 2004. Tie2/angiopoietin-1 signaling regulates hematopoietic stem cell quiescence in the bone marrow niche. *Cell.* 118: 149–161. http://dx.doi.org/10.1016/j.cell.2004.07.004

Bianco, P., S.A. Kuznetsov, M. Riminucci, and P. Gehron Robey. 2006. Postnatal skeletal stem cells. *Methods Enzymol.* 419:117–148. http://dx.doi.org/10.1016/S0076-6879(06)19006-0

Bianco, P., X. Cao, P.S. Frenette, J.J. Mao, P.G. Robey, P.J. Simmons, and C.Y. Wang. 2013. The meaning, the sense and the significance: translating the science of mesenchymal stem cells into medicine. *Nat. Med.* 19: 35–42. http://dx.doi.org/10.1038/nm.3028

Broxmeyer, H.E. 2011. Insights into the biology of cord blood stem/progenitor cells. *Cell Prolif.* 44:55–59. http://dx.doi.org/10.1111/j.1365-2184.2010.00728.x

Calvi, L.M., G.B. Adams, K.W. Weibrecht, J.M. Weber, D.P. Olson, M.C. Knight, R.P. Martin, E. Schipani, P. Divieti, F.R. Bringhurst, et al. 2003. Osteoblastic cells regulate the haematopoietic stem cell niche. *Nature.* 425:841–846. http://dx.doi.org/10.1038/nature02040

Chan, C.K., C.C. Chen, C.A. Luppen, J.B. Kim, A.T. DeBoer, K. Wei, J.A. Helms, C.J. Kuo, D.L. Kraft, and I.L. Weissman. 2009. Endochondral ossification is required for haematopoietic stem-cell niche formation. *Nature.* 457:490–494. http://dx.doi.org/10.1038/nature07547

Chou, S., P. Chu, W. Hwang, and H. Lodish. 2010. Expansion of human cord blood hematopoietic stem cells for transplantation. *Cell Stem Cell.* 7:427–428. http://dx.doi.org/10.1016/j.stem.2010.09.001

Delorme, B., J. Ringe, N. Gallay, Y. Le Vern, D. Kerboeuf, C. Jorgensen, P. Rosset, L. Sensebé, P. Layrolle, T. Häupl, and P. Charbord. 2008. Specific plasma membrane protein phenotype of culture-amplified and native human bone marrow mesenchymal stem cells. *Blood*. 111:2631–2635. http://dx.doi.org/10.1182/blood-2007-07-099622

Dexter, T.M., T.D. Allen, and L.G. Lajtha. 1977. Conditions controlling the proliferation of haemopoietic stem cells in vitro. *J. Cell. Physiol.* 91:335–344. http://dx.doi.org/10.1002/jcp.1040910303

Ding, L., T.L. Saunders, G. Enikolopov, and S.J. Morrison. 2012. Endothelial and perivascular cells maintain haematopoietic stem cells. *Nature*. 481:457–462. http://dx.doi.org/10.1038/nature10783

Dominici, M., K. Le Blanc, I. Mueller, I. Slaper-Cortenbach, F. Marini, D. Krause, R. Deans, A. Keating, Dj. Prockop, and E. Horwitz. 2006. Minimal criteria for defining multipotent mesenchymal stromal cells. The International Society for Cellular Therapy position statement. *Cytotherapy*. 8:315–317. http://dx.doi.org/10.1080/14653240600855905

Ferraro, F., S. Lymperi, S. Méndez-Ferrer, B. Saez, J.A. Spencer, B.Y. Yeap, E. Masselli, G. Graiani, L. Prezioso, E.L. Rizzini, et al. 2011. Diabetes impairs hematopoietic stem cell mobilization by altering niche function. *Sci. Transl. Med.* 3:104ra101. http://dx.doi.org/10.1126/scitranslmed.3002191

Frenette, P.S., S. Pinho, D. Lucas, and C. Scheiermann. 2013. Mesenchymal stem cell: keystone of the hematopoietic stem cell niche and a stepping-stone for regenerative medicine. *Annu. Rev. Immunol.* 31:285–316. http://dx.doi.org/10.1146/annurev-immunol-032712-095919

Friedenstein, A.J., R.K. Chailakhjan, and K.S. Lalykina. 1970. The development of fibroblast colonies in monolayer cultures of guinea-pig bone marrow and spleen cells. *Cell Tissue Kinet.* 3:393–403.

Houlihan, D.D., Y. Mabuchi, S. Morikawa, K. Niibe, D. Araki, S. Suzuki, H. Okano, and Y. Matsuzaki. 2012. Isolation of mouse mesenchymal stem cells on the basis of expression of Sca-1 and PDGFR-α. *Nat. Protoc.* 7:2103–2111. http://dx.doi.org/10.1038/nprot.2012.125

Kawamoto, T. 2003. Use of a new adhesive film for the preparation of multi-purpose fresh-frozen sections from hard tissues, whole-animals, insects and plants. *Arch. Histol. Cytol.* 66:123–143. http://dx.doi.org/10.1679/aohc.66.123

Kiel, M.J., O.H. Yilmaz, T. Iwashita, O.H. Yilmaz, C. Terhorst, and S.J. Morrison. 2005. SLAM family receptors distinguish hematopoietic stem and progenitor cells and reveal endothelial niches for stem cells. *Cell*. 121:1109–1121. http://dx.doi.org/10.1016/j.cell.2005.05.026

Kuznetsov, S.A., P.H. Krebsbach, K. Satomura, J. Kerr, M. Riminucci, D. Benayahu, and P.G. Robey. 1997. Single-colony derived strains of human marrow stromal fibroblasts form bone after transplantation in vivo. *J. Bone Miner. Res.* 12:1335–1347. http://dx.doi.org/10.1359/jbmr.1997.12.9.1335

Li, Q., Y. Yu, J. Bischoff, J.B. Mulliken, and B.R. Olsen. 2003. Differential expression of CD146 in tissues and endothelial cells derived from infantile haemangioma and normal human skin. *J. Pathol.* 201:296–302. http://dx.doi.org/10.1002/path.1443

Liu, H., K. Lu, P.A. MacAry, K.L. Wong, A. Heng, T. Cao, and D.M. Kemeny. 2012. Soluble molecules are key in maintaining the immunomodulatory activity of murine mesenchymal stromal cells. *J. Cell Sci.* 125:200–208. http://dx.doi.org/10.1242/jcs.093070

Meirelles, Lda.S., and N.B. Nardi. 2003. Murine marrow-derived mesenchymal stem cell: isolation, in vitro expansion, and characterization. *Br. J. Haematol.* 123:702–711. http://dx.doi.org/10.1046/j.1365-2141.2003.04669.x

Méndez-Ferrer, S., A. Chow, M. Merad, and P.S. Frenette. 2009. Circadian rhythms influence hematopoietic stem cells. *Curr. Opin. Hematol.* 16:235–242. http://dx.doi.org/10.1097/MOH.0b013e32832bd0f5

Méndez-Ferrer, S., T.V. Michurina, F. Ferraro, A.R. Mazloom, B.D. Macarthur, S.A. Lira, D.T. Scadden, A. Ma'ayan, G.N. Enikolopov, and P.S. Frenette. 2010. Mesenchymal and haematopoietic stem cells form a unique bone marrow niche. *Nature*. 466:829–834. http://dx.doi.org/10.1038/nature09262

Mercier, F.E., C. Ragu, and D.T. Scadden. 2012. The bone marrow at the crossroads of blood and immunity. *Nat. Rev. Immunol.* 12:49–60. http://dx.doi.org/10.1038/nri3132

Mignone, J.L., V. Kukekov, A.S. Chiang, D. Steindler, and G. Enikolopov. 2004. Neural stem and progenitor cells in nestin-GFP transgenic mice. *J. Comp. Neurol.* 469:311–324. http://dx.doi.org/10.1002/cne.10964

Morikawa, S., Y. Mabuchi, Y. Kubota, Y. Nagai, K. Niibe, E. Hiratsu, S. Suzuki, C. Miyauchi-Hara, N. Nagoshi, T. Sunabori, et al. 2009. Prospective identification, isolation, and systemic transplantation of multipotent mesenchymal stem cells in murine bone marrow. *J. Exp. Med.* 206:2483–2496. http://dx.doi.org/10.1084/jem.20091046

Nagoshi, N., S. Shibata, Y. Kubota, M. Nakamura, Y. Nagai, E. Satoh, S. Morikawa, Y. Okada, Y. Mabuchi, H. Katoh, et al. 2008. Ontogeny and multipotency of neural crest-derived stem cells in mouse bone marrow, dorsal root ganglia, and whisker pad. *Cell Stem Cell*. 2:392–403. http://dx.doi.org/10.1016/j.stem.2008.03.005

Naveiras, O., V. Nardi, P.L. Wenzel, P.V. Hauschka, F. Fahey, and G.Q. Daley. 2009. Bone-marrow adipocytes as negative regulators of the haematopoietic microenvironment. *Nature*. 460:259–263. http://dx.doi.org/10.1038/nature08099

Notta, F., S. Doulatov, E. Laurenti, A. Poeppl, I. Jurisica, and J.E. Dick. 2011. Isolation of single human hematopoietic stem cells capable of long-term multilineage engraftment. *Science*. 333:218–221. http://dx.doi.org/10.1126/science.1201219

Omatsu, Y., T. Sugiyama, H. Kohara, G. Kondoh, N. Fujii, K. Kohno, and T. Nagasawa. 2010. The essential functions of adipo-osteogenic progenitors as the hematopoietic stem and progenitor cell niche. *Immunity*. 33:387–399. http://dx.doi.org/10.1016/j.immuni.2010.08.017

Ozerdem, U., K.A. Grako, K. Dahlin-Huppe, E. Monosov, and W.B. Stallcup. 2001. NG2 proteoglycan is expressed exclusively by mural cells during vascular morphogenesis. *Dev. Dyn.* 222:218–227. http://dx.doi.org/10.1002/dvdy.1200

Phinney, D.G., G. Kopen, R.L. Isaacson, and D.J. Prockop. 1999. Plastic adherent stromal cells from the bone marrow of commonly used strains of inbred mice: variations in yield, growth, and differentiation. *J. Cell. Biochem.* 72:570–585. http://dx.doi.org/10.1002/(SICI)1097-4644(19990315)72:4<570::AID-JCB12>3.0.CO;2-W

Pittenger, M.F., A.M. Mackay, S.C. Beck, R.K. Jaiswal, R. Douglas, J.D. Mosca, M.A. Moorman, D.W. Simonetti, S. Craig, and D.R. Marshak. 1999. Multilineage potential of adult human mesenchymal stem cells. *Science*. 284:143–147. http://dx.doi.org/10.1126/science.284.5411.143

Sacchetti, B., A. Funari, S. Michienzi, S. Di Cesare, S. Piersanti, I. Saggio, E. Tagliafico, S. Ferrari, P.G. Robey, M. Riminucci, and P. Bianco. 2007. Self-renewing osteoprogenitors in bone marrow sinusoids can organize a hematopoietic microenvironment. *Cell*. 131:324–336. http://dx.doi.org/10.1016/j.cell.2007.08.025

Schajnovitz, A., T. Itkin, G. D'Uva, A. Kalinkovich, K. Golan, A. Ludin, D. Cohen, Z. Shulman, A. Avigdor, A. Nagler, et al. 2011. CXCL12 secretion by bone marrow stromal cells is dependent on cell contact and mediated by connexin-43 and connexin-45 gap junctions. *Nat. Immunol.* 12:391–398. http://dx.doi.org/10.1038/ni.2017

Schofield, R. 1978. The relationship between the spleen colony-forming cell and the haemopoietic stem cell. *Blood Cells*. 4:7–25.

Sugiyama, T., H. Kohara, M. Noda, and T. Nagasawa. 2006. Maintenance of the hematopoietic stem cell pool by CXCL12-CXCR4 chemokine signaling in bone marrow stromal cell niches. *Immunity*. 25:977–988. http://dx.doi.org/10.1016/j.immuni.2006.10.016

Takashima, Y., T. Era, K. Nakao, S. Kondo, M. Kasuga, A.G. Smith, and S. Nishikawa. 2007. Neuroepithelial cells supply an initial transient wave of MSC differentiation. *Cell*. 129:1377–1388. http://dx.doi.org/10.1016/j.cell.2007.04.028

Tanabe, S., Y. Sato, T. Suzuki, K. Suzuki, T. Nagao, and T. Yamaguchi. 2008. Gene expression profiling of human mesenchymal stem cells for identification of novel markers in early- and late-stage cell culture. *J. Biochem.* 144:399–408. http://dx.doi.org/10.1093/jb/mvn082

Tormin, A., O. Li, J.C. Brune, S. Walsh, B. Schütz, M. Ehinger, N. Ditzel, M. Kassem, and S. Scheding. 2011. CD146 expression on primary nonhematopoietic bone marrow stem cells is correlated with in situ localization. *Blood*. 117:5067–5077. http://dx.doi.org/10.1182/blood-2010-08-304287

Wang, L.D., and A.J. Wagers. 2011. Dynamic niches in the origination and differentiation of haematopoietic stem cells. *Nat. Rev. Mol. Cell Biol.* 12:643–655. http://dx.doi.org/10.1038/nrm3184

Zhang, J., C. Niu, L. Ye, H. Huang, X. He, W.G. Tong, J. Ross, J. Haug, T. Johnson, J.Q. Feng, et al. 2003. Identification of the haematopoietic stem cell niche and control of the niche size. *Nature*. 425:836–841. http://dx.doi.org/10.1038/nature02041